MATRIX DETERMINATION OF REFLECTANCE

OF HIDDEN OBJECT BY INDIRECT PHOTOGRAPHY

THESIS

Simon S. Ferrel, 2nd Lieutenant, USAF

AFIT/APPLPHY/ENP/12-M05

DEPARTMENT OF THE AIR FORCE
AIR UNIVERSITY

AIR FORCE INSTITUTE OF TECHNOLOGY

Wright-Patterson Air Force Base, Ohio

AFIT/APPLPHY/ENP/12-M05

MATRIX DETERMINATION OF REFLECTANCE OF HIDDEN OBJECT BY INDIRECT PHOTOGRAPHY

THESIS

Presented to the Faculty

Department of Engineering Physics

Graduate School of Engineering and Management

Air Force Institute of Technology

Air University

Air Education and Training Command

In Partial Fulfillment of the Requirements for the

Degree of Master of Science in Applied Physics

Simon S. Ferrel, BS

2nd Lieutenant, USAF

March 2012

AFIT/APPLPHY/ENP/12-M05

MATRIX DETERMINATION OF REFLECTANCE OF HIDDEN OBJECT BY INDIRECT PHOTOGRAPHY

Simon S. Ferrel, BS

2nd Lieutenant, USAF

Approved:

_____//SIGNED//_____	_____
Michael A. Marciniak, PhD (Chairman)	Date
_____//SIGNED//_____	_____
Mark E. Oxley, PhD (Member)	Date
_____//SIGNED//_____	_____
David E. Weeks, PhD (Member)	Date

Abstract

Indirect photography is a recently demonstrated technique which expands on the principles of dual photography and allows for the imaging of hidden objects. A camera and light source are collocated with neither having line-of-sight access to the hidden object. Light from the source, a laser, is reflected off a visible non-specular surface onto the hidden object, where it is reflected back to the initial non-specular surface and collected by the camera. This process may be repeated numerous times for various laser spot positions to yield slightly different camera images due to a variation in the illumination of the object. These images can then be used to construct an "indirect" image of the hidden object. This thesis provides an alternative method of processing the camera images by modeling the system as a set of transport and reflectance matrices. This approach reduces the required size of the visible scattering surface. Matrix formulation and those parameters shown in simulation to improve indirect image quality as measured by a modified MTF, including the method of matrix inversion, and number and pattern of laser spots, are discussed.

Acknowledgments

I would like to express my appreciation and gratitude for a number of people. First and foremost I would like to thank my faculty advisor, Dr. Michael Marciniak, for his time, support and expertise. Additionally, I would like to thank several members of the Department of Mathematics and Statistics at AFIT for their assistance, particularly Dr. Oxley and Dr. Fickus. Nathan Powell, Greg Smith and particularly 2nd Lieutenant Jessica Shafer were also of great assistance during the experimental work leading up to this research, and I am grateful to them for the assistance and knowledge.

Simon S. Ferrel

Table of Contents

Page

Abstract iv

Acknowledgments v

Table of Contents vi

List of Figures viii

List of Tables x

1 Introduction 1

1.1 Problem Statement 1
1.2 General Issue 1
1.3 Research Focus 3
1.4 Investigative Questions 4
1.5 Implications 5
1.6 Document Overview 6

2 Literature Review 7

2.1 Chapter Overview 7
2.2 Relevant Research 7
2.3 Summary 15

3 Methodology 16

3.1 Chapter Overview 16
3.2 Theory 16
3.3 Simulated Setup 21
3.4 Chapter Summary 24

4 Analysis and Results 25

4.1 Chapter Overview 25
4.2 Results of Simulation Scenarios 25
4.3 Investigative Questions Answered 45
4.4 Summary 46

5 Conclusions and Recommendations 47

5.1 Chapter Overview 47
5.2 Conclusions of Research 47
5.3 Significance of Research 48

5.4 Recommendations for Future Research 48
5.5 Recommendations for Action.....50
5.6 Summary 50

Appendix A – Representative Example of Simulation Code.....51

Bibliography 56

List of Figures

Figure Page

1. Indirect photography with camera field of view dictated by point of illumination 2
2. Indirect photography setup with fixed camera field of view.....3
3. Creating the transport matrix from data images (Hoelscher, 2011) 9
4. 5 of clubs indirect images at various resolutions (Hoelscher, 2011).....10
5. Prior experimental setup (Ferrel, Schafer, & Powell, 2011) 12
6. Checkerboards used as hidden object.....12
7. Example of camera image for experimental setup 13
8. Difference between ideal and recovered image (Ferrel, Schafer, & Powell, 2011) 14
9. Spatial coordinate system with respect to the three reflecting surfaces. 17
10. Different laser spot layouts.....23
11. Comparison of indirect images returned via Moore-Penrose pseudoinverse and mrdivide.....27
12. Modified MTF as a function of number of laser spots for 2x2 objects at different resolutions 29
13. Modified MTF as a function of number of laser spots for 4x4 objects at different resolutions 30
14. Modified MTF as a function of number of laser spots for 8x8 objects at different resolutions 31
15. Condition number as a function of number of laser spots.....33
16. Minimum eigenvalue as a function of number of laser spots.....34
17. Modified MTF as a function of laser spot distance from C 35
18. Recovered images at varying distances from C.....36

19. Cross-section of setup used in experimental and simulated trials 37

20. (Left) Modified MTF as a function of distance from C for two different patterns of laser spots; (Right) Laser spot patterns used 40

21. (Top) Contour map of matrix $\boldsymbol{G12}$ and (bottom) resulting images with and without stagger 41

22. Modified MTF of 2x2 Objects at Varying Resolution 42

23. Recovered indirect images for 2x2 object at 4x4 resolution with intensity added percent error 43

24. Recovered indirect images for 2x2 object at 8x8 resolution with intensity added percent error 44

List of Tables

Table Page

1. Modified MTF of 2x2 checkerboard with 64 resolution elements by method 26

2. ***K*** with laser spots 7.5” from C.....38

3. ***K*** with laser spots 1” from C.....39

4. ***K*** with laser spots 11” from C.....39

MATRIX DETERMINATION OF REFLECTIVITY OF HIDDEN OBJECT VIA INDIRECT PHOTOGRAPHY

1. Introduction

1.1 Problem Statement

The United States Air Force and other branches of the United States military constantly gather intelligence on unknown areas, both as a means to identify potential targets as well as to conduct reconnaissance before entering an area. While numerous methods currently exist to accomplish this, an adversary wishing to prevent friendly personnel from acquiring an image of an area merely needs to block the line of sight, thereby limiting the amount of intelligence available to the military. An ability to gather images from areas without a direct line of sight would be a great improvement. This paper discusses the possibilities and limits of using indirect photography, particularly in using a matrix formulation, as a technique to accomplish this goal.

1.2 General Issue

Dual photography is a relatively recent photographic technique which takes advantage of Helmholtz reciprocity to allow the positions of camera and illuminating light source to be interchanged (Sen *et al.*, 2005). Dual photography takes advantage of this to allow information which is available (or visible) to the light source, but not the camera, to be restored and captured by the camera. While an interesting advance with

great application in computer generated graphics, dual photography requires that the light source, in this case a pixilated projector, be placed in a position with a clear view of the object of which an image is desired. As a result, dual photography cannot be used to obtain imagery which is otherwise unavailable to either the light source or the camera. Indirect photography takes this one step further. As demonstrated by Lieutenant Colonel Mark Hoelscher, USAF, using multiple non-specular surfaces, it is possible to co-locate the camera and light source (in this case a laser), neither of which has a direct line of sight to the object in question, and still obtain recognizable visuals of that object, though not as clearly as can be accomplished via dual photography (Hoelscher, 2011). In indirect photography, one point on a surface (hereafter referred to as surface 1) is illuminated, causing non-specularly reflected light to be cast upon the object (also referred to here as surface 2) and then back to either the initial or some other surface (referred to here as surface 3). This, however, was accomplished by moving the field of view (FOV) of the camera and the light source as one unit on surfaces 1/3, which required a relatively large surface with an unchanging Bidirectional Reflectance Distribution Function (BRDF).

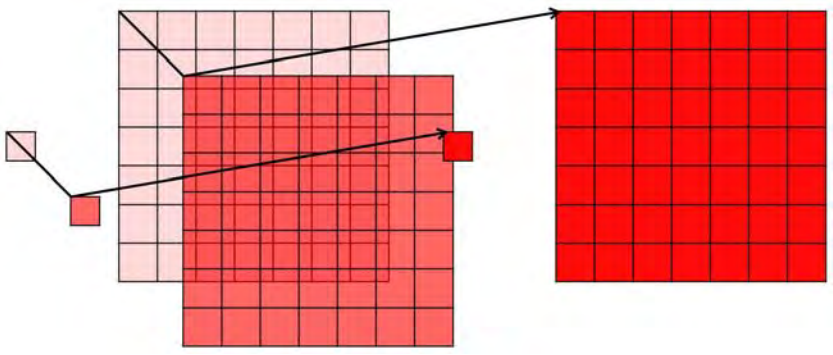

Figure 1. Indirect photography with camera field of view dictated by point of illumination.

1.3 Research Focus

In an effort to increase the practical application of indirect photography, this research focuses on the possibility of moving the light source, while keeping the camera FOV immobile. This results in a configuration, shown in Figure 2, where the laser spots are located around the camera field of view, thus reducing both the area needed, as well as the chances that the reflective properties differ at various locations of surface 1/3.

In this case, the large center grid again represents the pixilated field of view of the camera. Using this setup, this is constant for all trials and the laser spots, represented by the outer ring of smaller squares, are the only thing which changes between different trials.

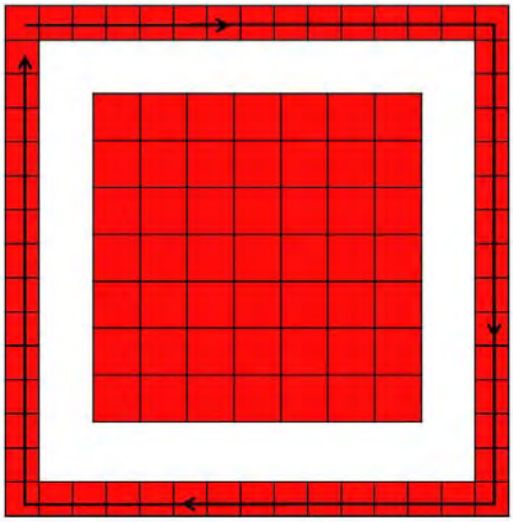

Figure 2. Indirect photography setup with fixed camera field of view.

This research also focuses on the matrix formulations of light transport in an effort to discover the general form of geometrical relationships between surfaces 1, 2 and

3, ideally leading to future work which will then be able to generalize appropriate approximations of these matrices for unknown geometries.

1.4 Investigative Questions

This research aims to answer several questions. The highest priority is to determine if it is possible to resolve an image of an object indirectly by using matrices as a means of representing the radiometric equations which have previously been developed (Hoelscher, 2011). This is more difficult than might be anticipated due to the nature of the matrices involved in this process. Because the dimensions of the matrices correspond to the number of laser spots used, the desired resolution of the object and the number of pixels in the camera, in most cases these matrices will not be square, making them non-invertible by simple means.

As a result, it is also important to determine which method of inverting non-square matrices should be used. Some possibilities include using the Moore-Penrose pseudoinverse or matrix right divide as defined in Matlab. If neither of these is effective, it will also necessitate more research to determine if other code will need to be written to perform the desired function.

Even after the preferred mathematical method is determined, many variables still remain which can affect how accurately an image can be resolved. These include the number of laser spots used to illuminate surface 1, as well as the general location and layout of these laser spots. Since the ideal number, location, and layout of laser spots will likely vary as a result of changing distances, angles and desired resolution, the first question in this area which needs to be answered is if there is a general trend in these

matters. Another important question is whether there is some sort of indicator which could be used to quickly find the ideal setup of laser spots, rather than having to repeatedly simulate any given situation to find the best setup.

All of this research is initially accomplished with a known geometry in order to best compare the resulting image with the original. However, as knowing the exact location and geometry of a hidden object is not realistic in most cases, another point of emphasis will be to understand the basic form which various matrices take in order to apply these to unknown geometries. This process was also intended to determine the importance of knowing an accurate geometry and the degradation of the image which occurs when the geometric relationship between surfaces is approximated, rather than known. This would also include an understanding of which values were important to know exactly and which can be estimated, as well as the effect when the geometry is incorrect or the data from the camera is flawed.

1.5 Implications

Research into indirect photography is still in its relative infancy. As a result, most practical applications will not be seen for quite some time. However, once enough research is completed, indirect photography will have major implications in a variety of fields, particularly to the military professional. With the current state of mobile computing, it is unlikely that this technique could be used regularly for immediate results. The delay involved in computing makes this more suitable to larger scale reconnaissance without immediate consequences (such as identifying if a particular vehicle is present in a covered hanger or not). Later, as computing power increases, indirect photography could

also be used on a personal level, enabling soldiers to see what awaits them around a corner. The techniques researched here could also be applied in similar situations by police officers, as well as by firefighters or other rescue workers in order to determine the locations of unconscious or otherwise incapacitated individuals.

1.6 Document Overview

This document contains a short summary of previous work in the field of indirect photography, as well as the principles upon which this work is based. Also included is a discussion of the research performed, both through experiment and simulation, including the specific geometries used for these. The data gathered from the experiment and multiple simulations is then analyzed to search for trends which may be used to determine the feasibility of using a matrix-based technique to determine the reflectance of a hidden object. This includes determining the effects of changing the number and position of these laser spots and surface 1, and the method of matrix inversion, as well as a brief discussion of the effect of incorrect measurements. This information is then used to draw conclusions about the feasibility of matrix-based determination techniques in indirect photography.

2. Literature Review

2.1 Chapter Overview

The purpose of this chapter is to give a brief insight into past research in the field of indirect photography and other relevant topics. Because indirect photography is relatively new, there has not yet been a great deal of research on this topic. While a brief overview of related research is included here, the dissertation "*Restoration of scene information reflected from non-specular media*" by Lieutenant Colonel Mark Hoelscher (Hoelscher, 2011) is recommended for a more in-depth treatment of the historical background leading up to indirect imaging.

Indirect photography is an adaptation of dual photography which relies on principles of Helmholtz reciprocity. As a result, the prior research considered here deals first very briefly with Helmholtz reciprocity, then transitions to dual photography, before touching briefly on the prior work in indirect photography accomplished by LtCol Hoelscher. In addition, because of the matrix nature of this research, a large amount of linear algebra is required, particularly relating to matrix inversion. For this reason, a brief discussion of matrix inversion will be included at the conclusion of this chapter.

2.2 Relevant Research

Helmholtz reciprocity states that light (or any electromagnetic radiation) can be reversed without changing the physics involved in its transportation. Initially Helmholtz only determined this to be the case for specular (mirrored) surfaces (von Helmholtz & Southall, 1862). However, Raleigh later expanded this to include non-specular media. (Rayleigh, 1900). He showed that given a single surface with an energy source situated

at any distance and at any angle from this surface, and a sensor also set at any distance and any angle (not necessarily the same distance and/or angle) from this surface, the source and the sensor can be interchanged and the sensor will still record the same measurement. This remained the case even if the light underwent reflection, refraction, or any other changes in path, so long as the polarization remained unchanged. This ability to mathematically change the locations of source and sensor led to the development of a technique referred to as dual photography (Sen *et al.*, 2005).

2.2.1 Dual Photography

Dual photography was initially pioneered in 2005 by Sen *et al*. with the intent of aiding in the creation of computer generated graphics. Though Helmholtz reciprocity was well understood previous to this time, these authors were able to apply this principle to allow images to be viewed from the locations of pixilated light sources. For a full understanding of dual photography, the reader is recommended *Dual Photography* by Sen *et al*. (Sen *et al.*, 2005).

The principles used in developing a transport matrix will receive a fuller treatment here, however, as these were applied in the current research as well. Given a projector with *p*x*q* pixel elements shining onto some surface and being photographed or otherwise viewed by a camera or sensor with *m*x*n* pixel elements, each element of the projector is lit up individually. This yields *p*x*q* trials, each of which are captured by every one of the camera's *m*x*n* pixel elements. The information collected by the camera from every trial is then combined as shown in Figure 3 to yield a matrix with *p*x*q* columns and *m*x*n* rows

representing a mapping of the flux from each of the *p*x*q* projector pixels to each of the *m*x*n* camera pixels.

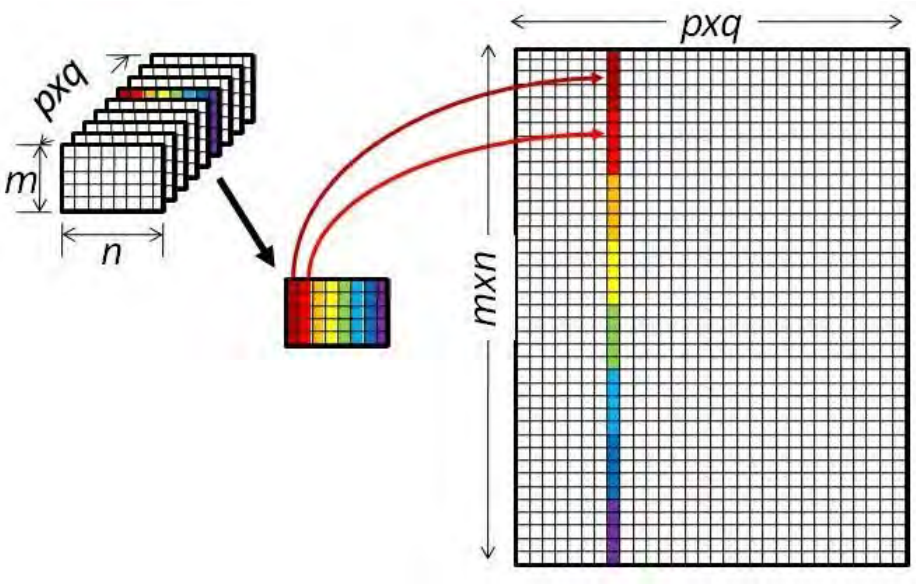

Figure 3. Creating the transport matrix from data images (Hoelscher, 2011).

The projected pattern is defined as a row vector with *p*x*q* columns and the camera images are defined as a column vector with *m*x*n* rows. Thus, the matrix representation is

$$c' = Tp' \tag{2.1}$$

where *c'* is the row vector of the camera images, *p'* is the row vector of the projected pattern and *T* is the transport matrix. The authors in the original paper formed a dual image simply by transposing *T* such that *p''* would be a virtual image formed at the projector given the camera projected a pattern *c''*. Note, however, that $TT^T \neq 1$. In this thesis, the inverse of *T*, T^{-1} will be required.

2.2.2 Indirect Photography

Indirect photography was introduced by LtCol Mark Hoelscher in 2011 in an effort to be able to gain access to information which is accessible by neither the camera nor the light source (Hoelscher, 2011). Here the idea of using a laser rather than a pixilated projector as the source of illumination was first introduced. These efforts met with considerable success, as evidenced in Figure 4.

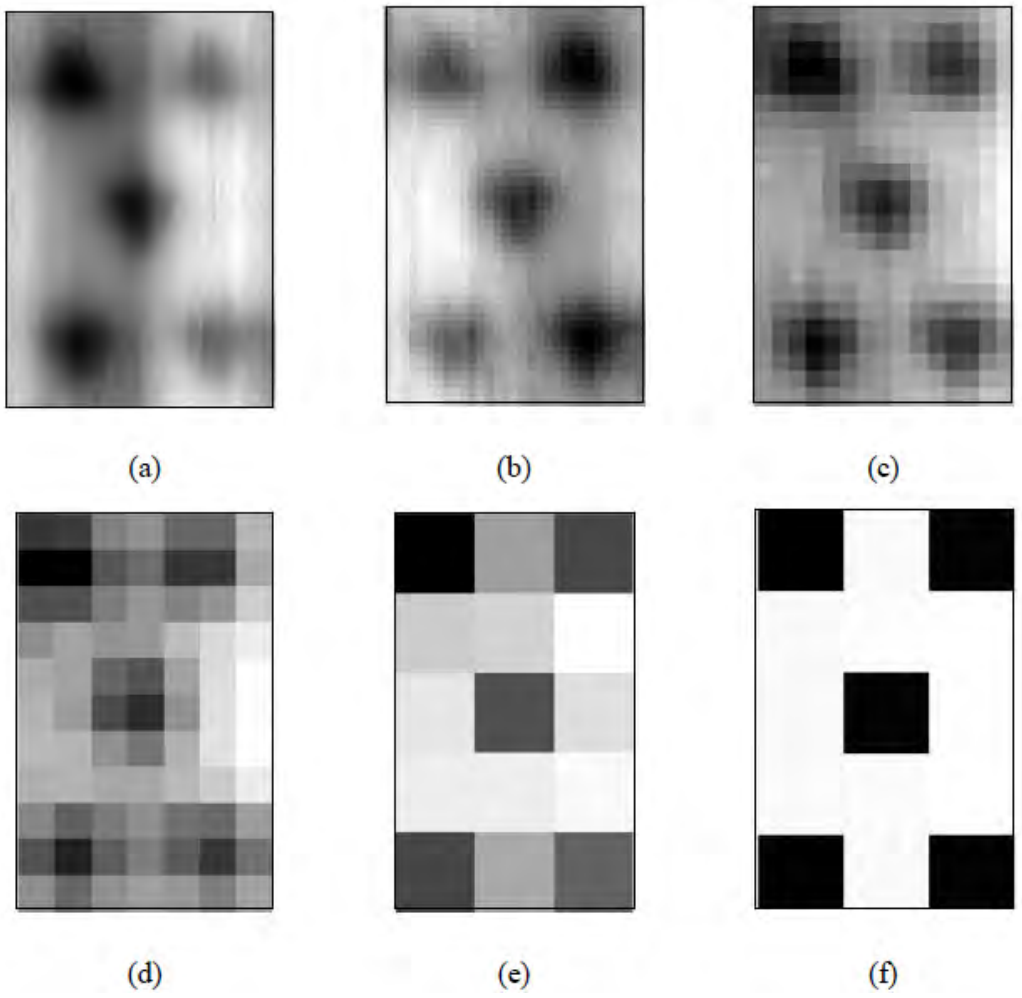

Figure 4. 5 of clubs indirect images at various resolutions (a) 95x63, (b) 47x31, (c) 23x15, (d) 11x7, (e) 5x3 and (f) 5x3 dual image (Hoelscher, 2011).

This research made the decision to collocate the laser and the camera so that the laser spot and the camera FOV would move together on surfaces 1/3. As it was no longer possible to simply determine T by observation, this would need to be modeled using radiometric principles. A large amount of the improvement in this process was due to the use of a blind deconvolution, which was only possible due to the fixed relationship between laser spot and camera FOV and the resulting form of the radiometric equations used. (Hoelscher, 2011).

In addition, this paper suggested using a matrix formulation as a means of revealing symmetries which might exist and aid in the deconvolution process. While this idea is not pursued in depth in his work, a matrix equation is suggested in equation (98) of the dissertation "*Restoration of scene information reflected from non-specular media*" (Hoelscher, 2011). Since a substantially different matrix formulation is applied here, the form suggested by LtCol Hoelscher is not included here, and those wishing to compare the two are suggested to review his work.

Additional work with an emphasis on a fixed camera FOV on surfaces 1/3 was also completed using data collected by Nathan Powell and analyzed by Lieutenants Simon Ferrel and Jessica Shafer (Ferrel, Schafer, & Powell, 2011). The experimental setup included a helium neon laser, two adjustable mirrors, two non-specular reflecting surfaces, and a digital camera, arranged as shown in Figure 5. The laser was designed to be incident upon various locations on the surface marked as surface 1, and was controlled by changing the angle of the mirrors in the system. The hidden object was placed face-down on surface 2, and the camera was situated to take a photograph of surface 3.

Though surface 1 and surface 3 were collocated in this case, the location of the incident laser spots was kept out of the field of view by approximately 2".

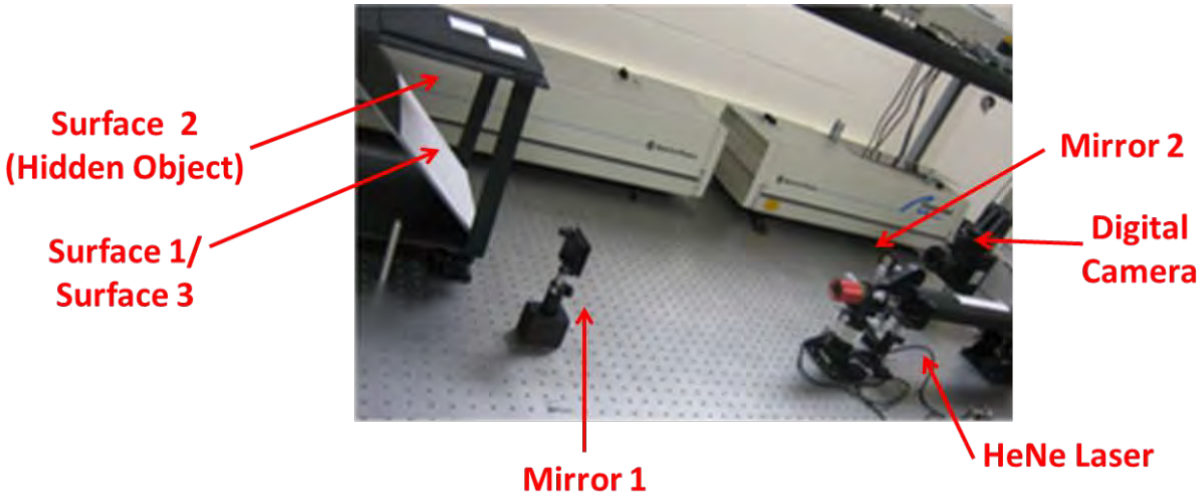

Figure 5. Prior experimental setup (Ferrel, Schafer, & Powell, 2011).

The laser light was reflected first off the two mirrors before hitting the first surface, then was reflected off of the second surface containing an object hidden from the camera. In an effort to determine the resolving power of indirect photography techniques for this setup, the hidden objects which were used were four black and white checkerboards of increasing spatial frequency as shown in Figure 6.

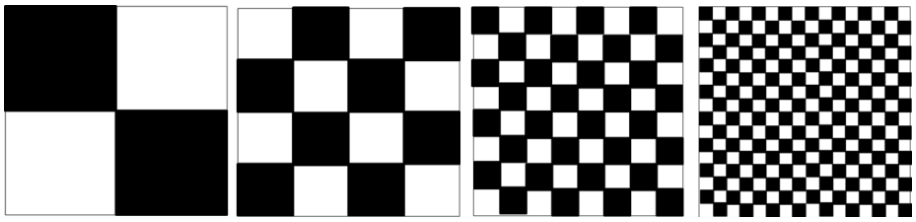

Figure 6. Checkerboards used as hidden object.

From this hidden object, the light was then reflected once more off of surface 3. The camera finally collected the light reflected from surface 3 which was within its field of view. An example of such a photograph is shown in Figure 7.

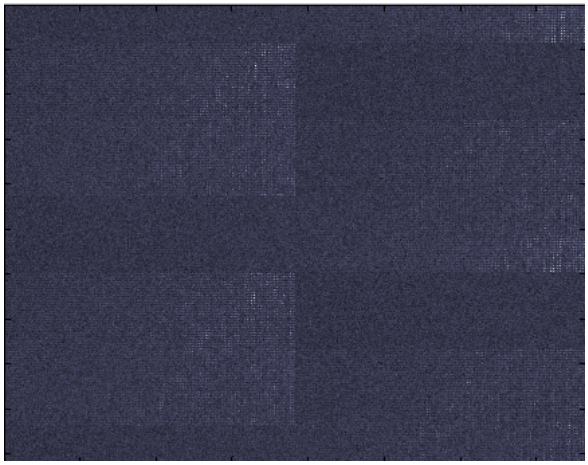

Figure 7. Example of camera image for experimental setup.

This process was repeated a total of 252 times, varying the position of the laser spot slightly. 61 laser spots were located along the bottom of the FOV, with an additional 63 on each side, and 65 on the top, all spaced approximately equally along these spaces. Each laser spot presented a slightly different illumination of the object, and thus, a slightly different image to the camera. Combining the images from all these trials as previously described in Figure 3 yielded the intensity matrix used in this case.

Unfortunately, no recognizable images could be recovered from the experimental data regardless of the spatial frequency of the hidden object or the method used for matrix inversion. One representative example of this is shown in Figure 8 for an attempt to resolve a 2x2 checkerboard at 8x8 resolution using the Moore-Penrose pseudoinverse.

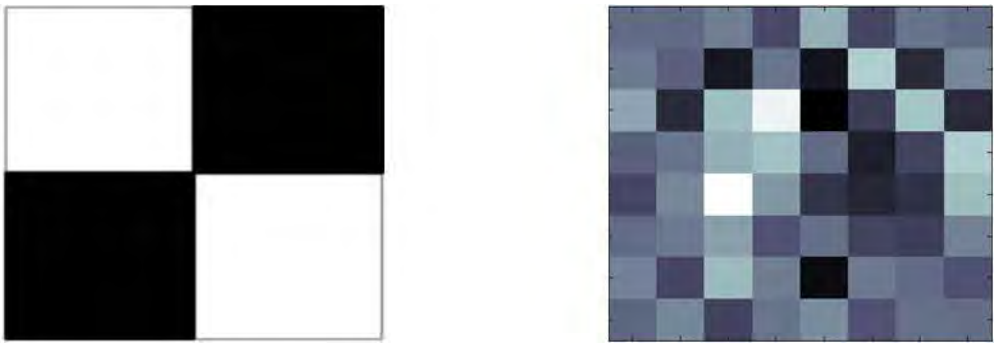

Figure 8. Difference between ideal image (left) and recovered image (right) in experimental results using the Moore-Penrose pseudoinverse.

While the matrix inversion resulted in some data being irretrievably lost, the main difficulties were a result of backscatter from the incident laser light. This was a result of the very low intensities of the multiply reflected light which actually contains the object information. While the light spots were outside the camera FOV, some light was reflected back off surface 1 into the internal workings of the camera. While this light was not directly imaged onto the CCD in the camera, scatter off the lens and internal workings of the camera was of equal or greater magnitude than the light containing object information and was processed into the images.

2.2.3 Linear Algebra

Given an *m*x*n* matrix *A*, with $m \neq n$, there is no generalized inverse A^{-1} such that $AA^{-1} = I_m$ and $A^{-1}A = I_n$, where I_m and I_m are the identity matrices. For the cases that the square matrices A^TA and AA^T are invertible there does exist a left inverse $A_{left}^{-1} = (A^TA)^{-1}A^T$ for matrices with $m > n$ and a right inverse $A_{right}^{-1} = A^T(AA^T)^{-1}$ for matrices with $m < n$. Because these are limited to cases where the matrix is not rank deficient, the Moore-Penrose pseudoinverse, $A^{\dagger}$, was developed, which always exists,

coincides with left, right and general inverses when they exist, and has the following properties (Penrose, 1955):

- $AA^{\dagger}A = A$
- $A^{\dagger}AA^{\dagger} = A^{\dagger}$
- $(AA^{\dagger})^{*} = AA^{\dagger}$
- $(A^{\dagger}A)^{*} = A^{\dagger}A$

(2.2)

This is particularly useful for cases where the same algorithm needs to be applied regardless of the dimensions of a given matrix. Another method of matrix inversion involves using the matrix right divide, mrdivide, command in Matlab, which solves the matrix equation $A = XB$ for X with as few non-zero elements as possible (Leon, 2005).

2.3 Summary

There has been very limited research in the field of indirect photography, and this research has occurred only recently. Additionally, while the work performed here does build upon previous advancements in understanding Helmholtz reciprocity, dual photography, indirect photography, and linear algebra, it nonetheless differs substantially from past efforts in these fields.

3. Methodology

3.1 Chapter Overview

This experiment was conducted in simulation using Matlab. This research was modeled after the experimental trial using fixed camera FOV on surface 1 as discussed in Chapter 2. (Ferrel, Schafer, & Powell, 2011). This involved creating a simulation with surfaces 1/3 and 2 in a specific configuration, and testing the effects on the returned indirect image which resulted from varying the number, location and layout of laser spots on surface 1.

3.2 Theory

The radiometric equation for radiance, from which all other radiometric quantities can be derived, is given by the spectral flux radiated per projected unit area of the source per detector solid angle, or

$$L_e = \frac{\partial^2 \phi_e}{\partial A_s cos\theta_s \partial \Omega_d} (\text{W cm}^{-2}\text{sr}^{-1}) \tag{3.1}$$

where $\partial \phi_e$ is the differential flux, $\partial A_s cos\theta_s$ is the differential projected area of the source, and $\partial \Omega_d$ the differential solid angle subtended by the detector. Rearranging terms in this equation and performing various operations give the other radiometric quantities, including flux, intensity, exitance, and irradiance (Dereniak & Boreman, 1996).

Given this, if the initial irradiance is known, so long as the geometry terms and BRDFs are understood, the reflected radiance and subsequent irradiance onto other surfaces may both be found after arbitrarily many reflections. Indirect photography

involves three occasions in which surfaces are impacted by light. The setup studied here is shown in Figure 9.

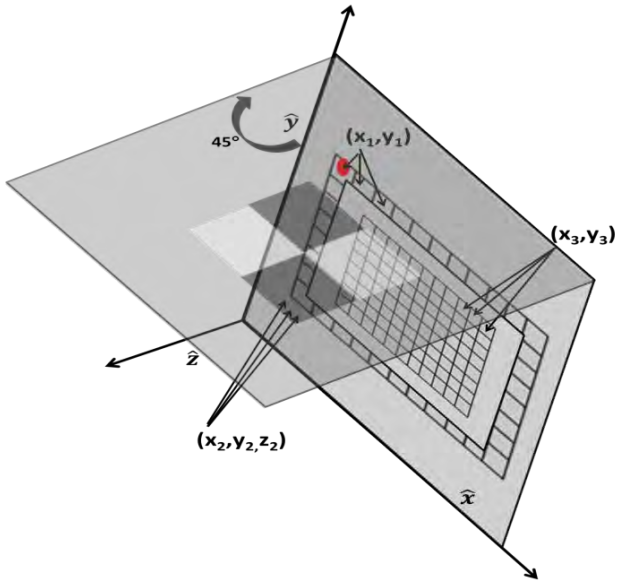

Figure 9. The spatial coordinate system with respect to the three reflecting surfaces.

The coordinates (x_1,y_1) correspond to the positions of the initial laser spots on surface 1. Coordinates (x_2,y_2,z_2) refer to a grid of locations on the hidden object found on surface 2, while (x_3,y_3) describe the grid of locations on the surface 3 (which in this case is the same as surface 1) within the camera's field of view. In all cases, the Cartesian origin was chosen to be the lower left corner of surface 1.

The proportion of flux which reaches surface 2 from surface 1 depends on the BRDF of surface 1 with respect to surface 2 (Driggers, Cox, & Edwards, 1999) and is proportional to

$$\left[\frac{\cos\theta_{d12}\cos\theta_{s12}}{R_{12}^2}\right] \odot [BRDF_{12}(\theta_{i1}, \theta_{s12}, \Delta\emptyset_{12})] \tag{3.2}$$

where $\theta_{d12}$is the zenith angle between a point on surface 1 (S1) and a point on surface 2 (S2) with respect to the normal of S2. $\theta_{s12}$is the zenith angle between a point on surface 1 (S1) and a point on surface 2 (S2) with respect to the normal of S1. R_{12} is the distance between these two points. $[BRDF_{12}(\theta_{i1}, \theta_{s12}, \Delta\emptyset_{12})]$ is the matrix of BRDFs of points on S1 to points on S2, which depends on the incident angle θ_{i1}, the zenith angle between the source and a point on S1 with respect to the normal of S1, $\theta_{s12}$and $\Delta\emptyset_{12}$, the azimuthal angle between the projection of the source ray onto S1 and the projection onto S1 of the ray between points on S1 and S2. $\odot$ is the Hadamard product, commonly known as point-wise matrix multiplication (Hogban, Brualdi, Greenbaum, & Matthias, 2003).

Similarly, the proportion of flux which reaches surface 3 and then the camera from surface 2 is given by

$$\left[\frac{\cos\theta_{d23}\cos\theta_{s23}}{R_{23}^2}\right] \odot [BRDF_{23cam}(\theta_{d23}, \theta_{s3cam}, \Delta\emptyset_{3cam})] \odot [BRDF_{123}(\theta_{d12}, \theta_{s23}, \Delta\emptyset_{23})] \tag{3.3}$$

with similar notation as Equation (3.2). Here, the subscripts on BRDF indicate position on the surface that is the source of the irradiance, the reflecting surface being considered, and position on surface collecting the reflected radiance, respectively. It should be noted that in both these equations, $\cos\theta_{d23}$, $\cos\theta_{s23}$ and R_{23} are dependent upon the exact location of the resolution element on surface 2 and camera FOV pixel on the surface 3,

and thus take different values for every camera pixel and every resolution element of the hidden object. Similarly, $\cos\theta_{d12}$, $\cos\theta_{s12}$ and R_{12} take unique values for every laser spot position and every resolution element of the hidden object.

This allows this total series of laser spot movement for the system of experiments shown in Figure 9 to be represented by the following matrix system:

$$[\Phi_{cam}] = \Phi_{laser} A_{s2} A_{lens} \Omega_{FOV} \left\{ [BRDF_{23cam}] \odot [BRDF_{123}] \odot [cos\theta_{d23}] \odot [\cos\theta_{s23}] \odot \left[\frac{1}{R_{23}^2}\right] \right\} * \left\{ \left[\frac{1}{R_{12}^2}\right] \odot [BRDF_{12}] \odot [\cos\theta_{d12}] \odot [cos\theta_{s12}] \right\} \quad (3.4)$$

where $[\Phi_{cam}]$ is a matrix the flux measured by the camera for any pixel at S3 for any laser spot position on S1, Φ_{laser} is the laser flux, A_{s2} is the resolution area defined on S2, A_{lens} is the area of the camera lens, Ω_{FOV} is the solid angle FOV of each camera pixel, and $*$ denotes the Kroenecker product, which is a general matrix multiplication (Hogban, Brualdi, Greenbaum, & Matthias, 2003). Φ_{laser}, A_{s2}, A_{lens}, and Ω_{FOV} are considered constants in these experiments. Since the absolute magnitude of $[\Phi_{cam}]$ is unimportant, these four can be considered to just scale $[\Phi_{cam}]$ and therefore removed from the equation.

In order to further simplify Equation (3.4), the assumption is made that the surfaces 1 and 3, upon which the laser light will be incident, are approximately Lambertian and therefore perfectly diffuse. While this is not exactly the case, this approximation will allow $BRDF_{23cam}$ and $BRDF_{12}$ to be approximated as constants.

Additionally $BRDF_{123}$is a three dimensional matrix because it accounts for the laser spot positions on S1, the resolution elements on S2, and the individual pixel locations of the camera's FOV on S3. Since solution of Equation (3.4) only allows for a two dimensional matrix $BRDF_{123}$, the assumption must be made that the BRDF at any position on S1 for any reflectance angle to S3 is the same regardless of the incident angle from S1. This is a good assumption for a Lambertian surface. Because of this, the only non-constant terms remaining in this matrix equation are those geometry terms which depend on the separations and angles between various points, as well as $BRDF_{123}$, which represents the object. Therefore, Equation (3.4) simplifies to

$$[\Phi_{cam}] \propto \{[BRDF_{123}] \odot [G_{23}]\} * [G_{12}] \tag{3.5}$$

where $[G_{23}]$ represents the geometric terms between the resolution points on surface 2 and the pixels of the camera FOV on surface 3, and is given by

$$[G_{23}] = [cos\theta_{d23}] \odot [\cos \theta_{s23}] \odot \left[\frac{1}{R_{23}^2}\right] \tag{3.6}$$

with all matrices of dimension *p*x*r* where *p* is the number of camera pixels and *r* the number of resolution elements. Similarly, $[G_{12}]$ represents the geometric relationship between the laser spots on surface 1 and the resolution points on surface 2, and is given by

$$[G_{12}] = [cos\theta_{d12}] \odot [\cos \theta_{s12}] \odot \left[\frac{1}{R_{12}^2}\right]. \tag{3.7}$$

with all matrices of dimension *r*x*l* where *r* is again the number of resolution elements and *l* corresponds to the number of laser spots used. These dimensions cause the recorded flux matrix $[\Phi_{cam}]$ to have dimensions *p*x*l*, which matches the method shown in Figure 3 for creating this matrix. While some of these geometric terms are generally unknown, in this particular experiment it is possible to measure them as a result of knowing locations of all points of interest. As a result, the BRDF of the unseen object can theoretically be determined using matrix manipulation. This requires first that an inverse be found for $[G_{12}]$, so that $[\Phi_{cam}]$ can be multiplied by it to give

$$[\Phi_{cam}] * [G_{12}]^{-1} \propto [BRDF_{123}] \odot [G_{23}] \tag{3.8}$$

Following this, $[G_{23}]$ is easily accounted for by simply taking the entry-wise reciprocal and multiplying both sides by that matrix. Since this step does not introduce additional uncertainty, the majority of the mathematical research done in this case centers on the inversion of $[G_{12}]$.

3.3 Simulated Setup

The simulation was modeled after the setup used by Ferrel, Schafer and Powell described in Chapter 2 and with schamtic shown in Figure 9 (Ferrel, Schafer, & Powell, 2011). In this case, the angle between surface 1/3 and surface 2 is 45 degrees, with surface 1/3 having a total length of 15.5” and a width of 11.5”. The hidden object was placed on surface 2, with the rear-most portion of the image 5.87” from the position where surface 2 intersects surface 1. The camera FOV remained in the same position regardless of location of the laser spot. Though the camera itself had a rectangular FOV,

due to the angle of surface 1/3, the FOV measured 4” in both the x-direction (up the board) and the y-direction (across the board), with the lower-left corner of the FOV located at coordinates corresponding to 3.25” in the x-direction and 2.75” in the y-direction.

In an effort to determine the resolving power of indirect photography techniques for this setup, the hidden objects which were used were the same four black and white checkerboards of increasing spatial frequency shown in Figure 6. Each of these checkerboards was of size 2”x2”, with the rear-most portion of the checkerboard 5.87” directly above S1 and the front of the checkerboard 9.87” above S1. The Matlab code used to model these positions, as well as the position of the laser spots, can be found in Appendix A.

Because these trials were accomplished in simulation, rather than being able to simply photograph the resulting intensity on surface 3, the matrix equation found in Equation (3.5) was used to determine the intensity that would be photographed by a camera in the ideal case. This implies that there are no aberrations or any other factors which disturb the transport of light except for the non-specular reflection at the three surfaces. While this is not entirely realistic, it is useful in evaluating the fundamental capabilities and limitations of matrix-based formulations of indirect photography.

The quality of the resulting indirect images is quantified by the modified Modulation Transfer Function (MTF) introduced by LtCol Hoelscher as:

$$MTF = \frac{White - Black}{White + Black} \tag{3.9}$$

where *White* is the average reflectance of all pixels in a recovered indirect image which correspond to the white pixels of the object and *Black* is the average reflectance of all pixels in a recovered indirect image which correspond to the black pixels of the object (Hoelscher, 2011). An MTF of -1.0 would be the exact opposite image of the object, an MTF of 0.0 would show no resolution of the objects spatial features and an MTF of 1.0 would be a perfect image of the object. MTF values less than -1.0 or greater than 1.0 can only occur mathematically in the case that some pixels take negative reflectance values, which is not physical.

This evaluation via MTF occurred for four different variables modified in Matlab code. These were (1) changing how the pseudoinverse of a matrix is calculated, (2) changing the number of laser spots on surface 1, (3) changing the distance that the laser spots are from the camera field of view on surface 1/3 and (4) changing how the laser spots are arranged at that distance. An example of two different laser spot layouts is shown in Figure 10.

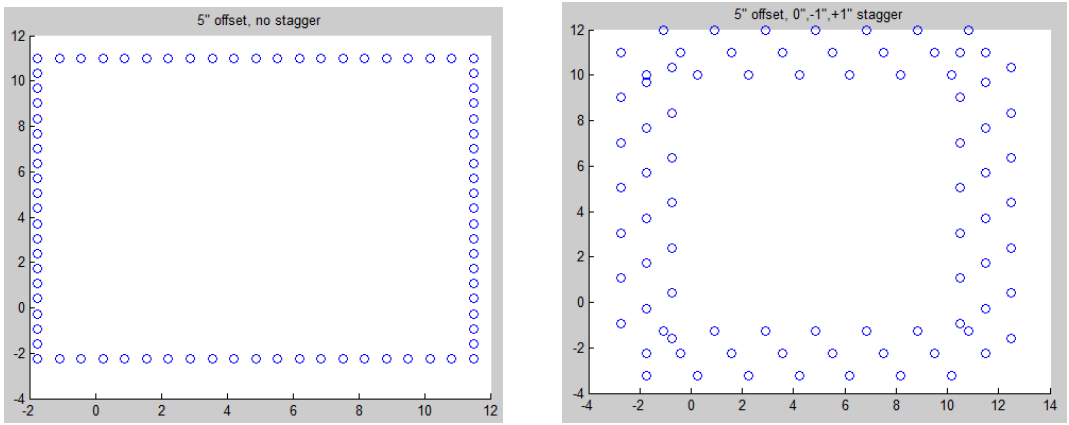

Figure 10. Different laser spot layouts.

Additionally some analysis was made of the effect of small errors in the data recorded by the camera, by purposely introducing a random normal percent error with varying standard deviation to the correctly derived intensity. All of these variables were not changed simultaneously in an effort to determine an overall best-case scenario as the currently available computing power made it infeasible to consider every possible permutation of these. Instead, each is considered individually in the hopes of unearthing general trends.

While a variety of different Matlab code was used in changing these different variables, one representative example is included in Appendix A.

3.4 Chapter Summary

The experiment described in Chapter 2 and the simulated portion of this research both use the same geometry, setup and equations, have different purposes. The experiment was designed to both test the real-world application of matrix-based techniques of indirect photography and expose any fundamental issues with the design of the experiment. Its immediate limitation, described in Chapter 2, prompted this research to be conducted via simulation, which allows for more trials as well as serves to remove extraneous variables which might make it more difficult to gain an understanding of the fundamental concepts involved in using matrices to perform indirect photography.

4. Analysis and Results

4.1 Chapter Overview

In simulation, a matrix-based technique for indirect imaging was shown to recover recognizable images. The quality of these images varied greatly depending on the desired resolution and the various controllable aspects of the setup, such as method of matrix inversion, and number of laser spots and the location/layout of laser spots on surface 1. General trends were found as to which setups would be the most effective, and multiple efforts were made to find an indicator, such as condition number or eigenvalue of the $[G_{12}]$ matrix, which would show which setup is most effective without requiring multiple simulation runs. All possible attempts at this showed no correlation to the effectiveness in resolving the image. Nonetheless, these general trends give some insight as to methods of improving images acquired via indirect photography.

4.2 Results of Simulation Scenarios

A number of variables, all of which are under user control, were considered in trying to maximize the modified MTF, as defined by Equation (3.9), of the acquired image. These included the method of matrix inversion, as well as the number and positions of the laser spots on surface 1. Additionally, simulation was performed to determine the effect of small errors in flux as measured by the camera. Because of computing power, these variables could not be considered jointly, but each is considered individually and yields usable information and a general trend.

4.2.1 Testing Method of Matrix Inversion

There are two different ways to solve the matrix equation $A = XB$ when B is a non-square matrix. This does not include using the right inverse $B_{right}^{-1} = B^T(BB^T)^{-1}$. Since the Moore-Penrose pseudoinverse is equal to the right matrix inverse when the right inverse exists, testing using the Moore-Penrose pseudoinverse makes testing indirect image quality using the right matrix inverse unnecessary. Using the Moore-Penrose pseudoinverse minimizes the Euclidean norm for $A - XB$, whereas using the mrdivide Matlab command solves with as sparse a matrix as possible. The more effective method is not initially obvious, especially when only considering the modified MTF, where 1.0 is ideal. Table 1 compares the modified MTF accomplished by each of these methods for resolution of a 2x2 checkerboard with 64 resolution elements using an increasing number of laser spots.

Table 1. Modified MTF of 2x2 checkerboard with 64 resolution elements by method

# of laser spots	Moore-Penrose	mrdivide
80	0.9714	0.9208
400	0.9772	0.9822
4000	0.9578	0.9705

By this comparison, the two methods seem to be similarly effective. However, in viewing the images returned by each of these methods, shown in Figure 14, it is obvious that the mrdivide images do not correspond to the MTF values assigned to them.

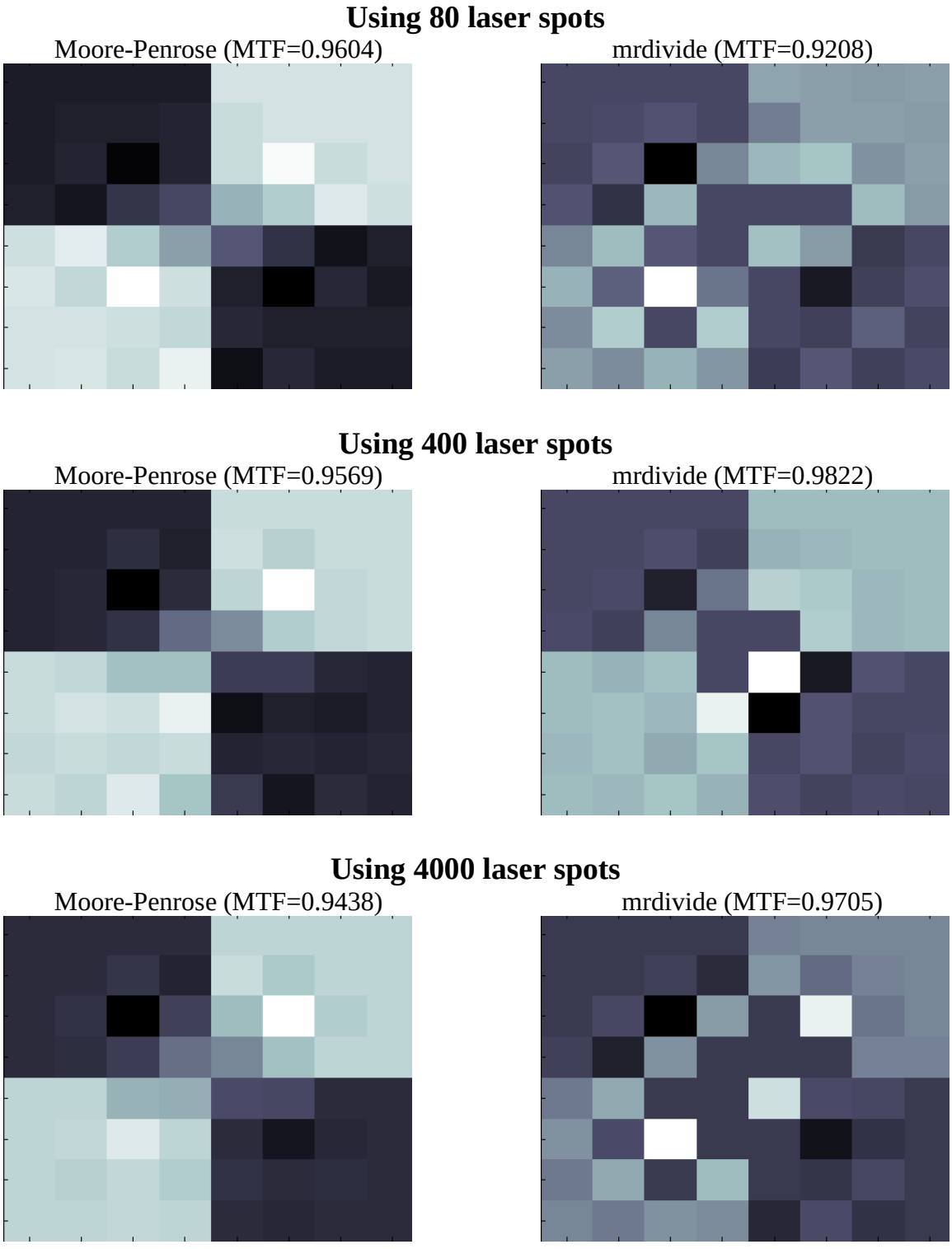

Figure 11. Comparison of indirect images returned for 2x2 checkerboard objects via Moore-Penrose pseudoinverse and mrdivide.

This disparity between image quality and assigned MTF value is a result of mrdivide returning negative reflectance values, which are non-physical (Meyer-Spradow & Loviscach, 2003). The Moore-Penrose pseudoinverse does not yield negative values as solution to this matrix system and is the preferred method for accurately resolving the image, regardless of the spatial frequency of the object or desired resolution of the resulting indirect image. For this reason, all remaining tests are done with matrix inversion accomplished via the Moore-Penrose pseudoinverse.

4.2.2 Testing Differing Number of Laser Spots

One of the other variables which can be adjusted from the position of the operator at the collocated camera and laser is the number of laser spots used for illumination, which corresponds to the number of experiments performed in order to obtain an indirect image. Because each laser spot used increases the number of trials and therefore the dimensions of several matrices involved in the calculation, it is advisable to use as few laser spots as possible to resolve a clear image. The ideal number of laser spots depends both on the spatial frequency of the object, as well as the desired resolution, as can be seen in Figures 12-14, where all trials were performed with the laser spots equally spaced in a 6”x6” square pattern centered on the point on S1 directly beneath the center of the hidden object. The 16x16 objects are not included since they cannot be recognizably resolved regardless of laser spot setup. In viewing these images, it must be noted that these results are specific to the geometry used in these simulated trials and that the ideal number of laser spots will likely vary with the setup.

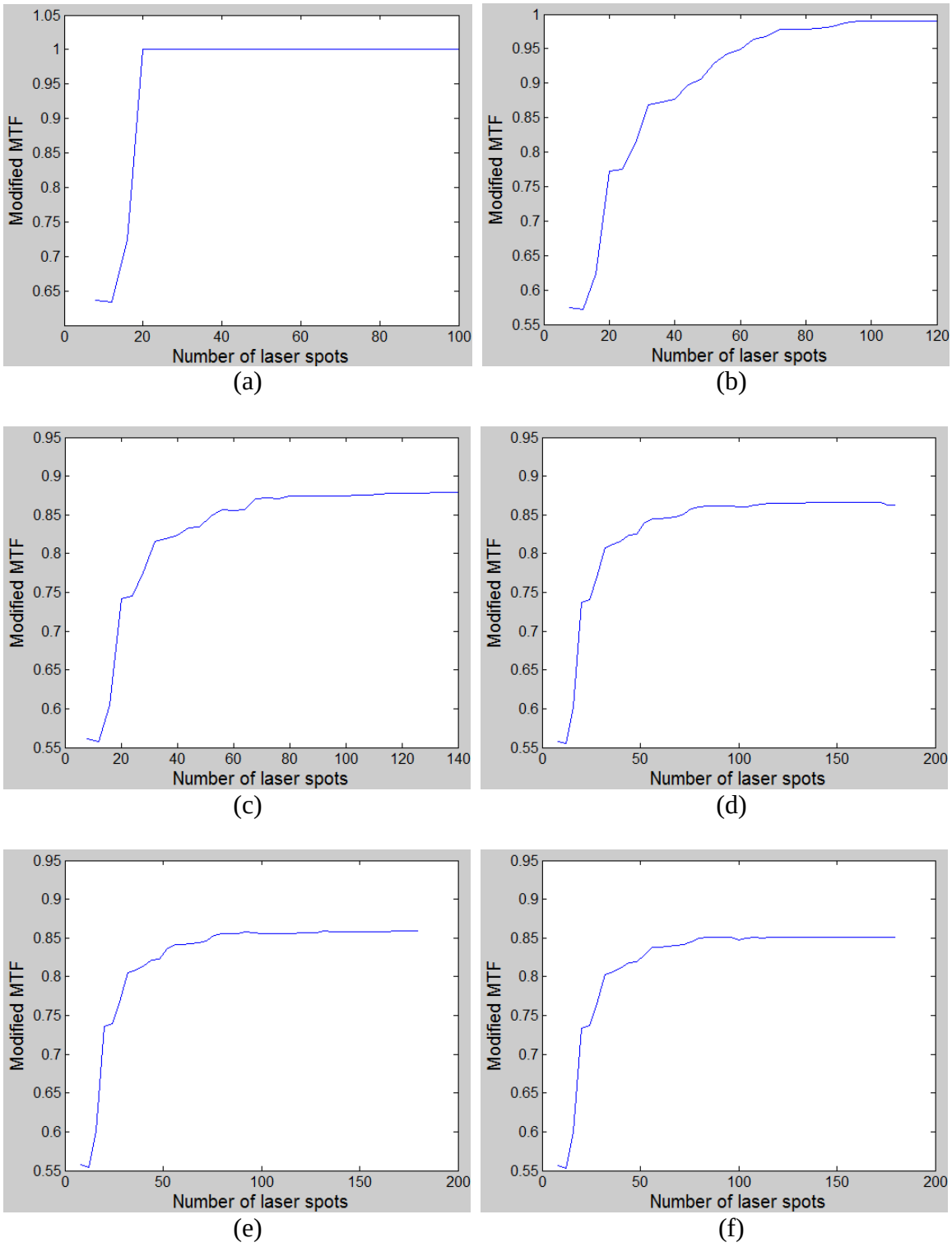

Figure 12. Modified MTF as a function of number of laser spots for 2x2 objects at different resolutions: (a) 4x4, (b) 8x8, (c) 16x16, (d) 24x24, (e) 32x32 and (f) 64x64.

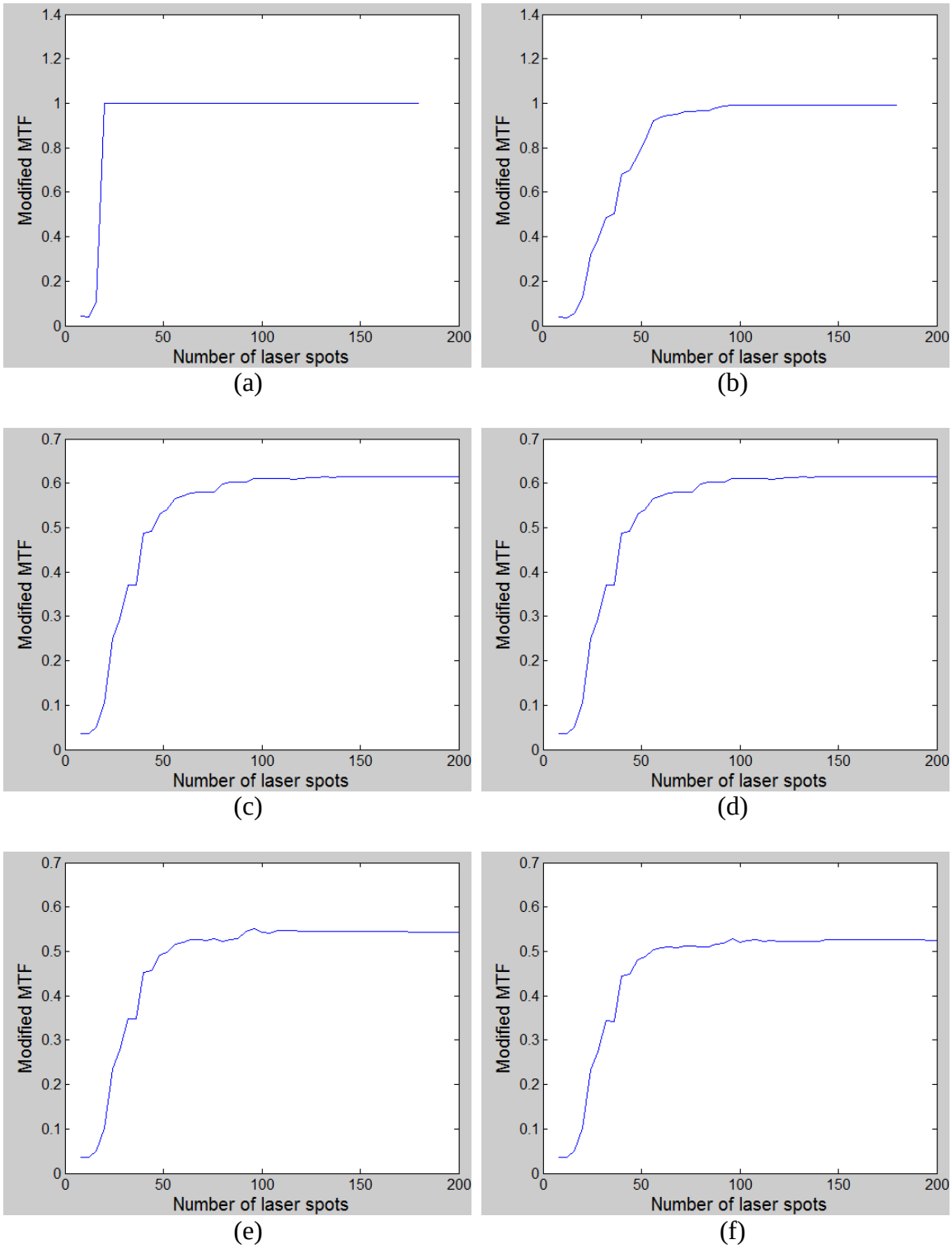

Figure 13. Modified MTF as a function of number of laser spots for 4x4 objects at different resolutions: (a) 4x4, (b) 8x8, (c) 16x16, (d) 24x24, (e) 32x32 and (f) 64x64.

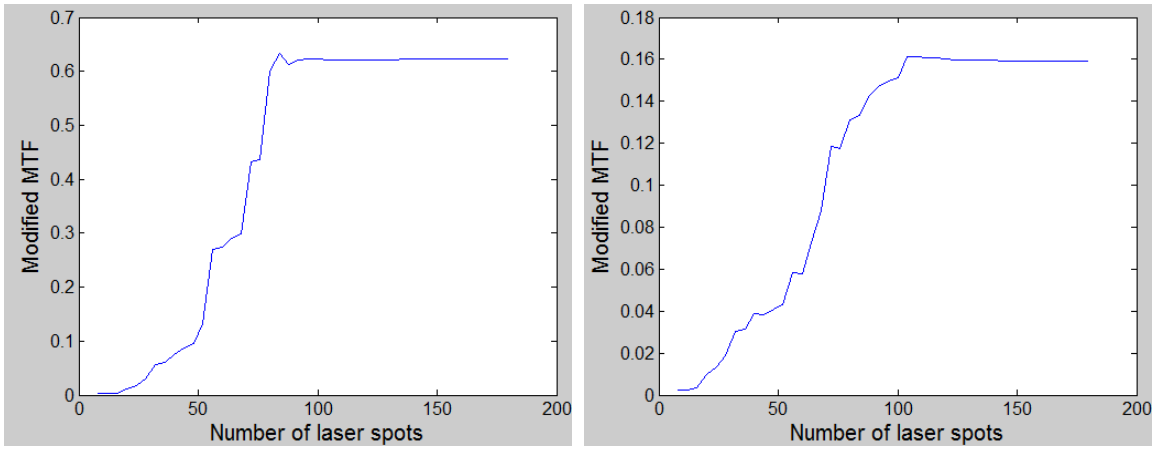

(a) (b)

Figure 14. Modified MTF as a function of number of laser spots for 8x8 objects at different resolutions.

Generally, however, it may be noted that modified MTF increases with the number of laser spots before leveling off, and that a higher desired resolution will require the use of more laser spots in order to achieve a similar quality of indirect image. It may also be noted that, for each spatial frequency checkerboard, the value of the modified MTF tends to level off, regardless of the desired resolution. This may be indicative of the laser spots being so near one another as to no longer give substantially different angles of illumination on the object and information.

Because this portion of the experiment was conducted entirely in simulation, the only cause of recovered images differing from the actual object is the data lost due to the necessary inversion of a geometrical matrix to solve for the indirect image of the object. Since this matrix's dimensions and values change as the number and layout of the laser spots change, ideally some characteristic of this matrix should change in relation to the

MTF of the recovered images, enabling this characteristic to serve as an indicator to select the best setup of laser spots.

The condition number of a matrix is defined as the ratio of the maximum and minimum eigenvalues of a matrix (Erceg, Soma, Baum, & Paulraj, 2002) and is equal to the norm of a matrix multiplied by the norm of the matrix inverse, or pseudoinverse in this case. Though condition number of this matrix, which is independent of the object, was tested as a possible indicator of ideal setup, there was no discernible pattern to the condition number, as shown in Figure 15. Condition number also serves as a measure of sensitivity of the solution, or how error in output (in this case, the image of the object) increases as a function of error in input (in this case, the data measured by the camera). Inversion by a matrix with a condition number of 1 does not increase the error, whereas a matrix with a larger condition number will require more initial accuracy. A large condition number also indicates that the matrix is less invertible. Given the very large condition numbers seen in Figure 15, particularly at higher resolutions, this is a serious concern and is addressed in section 4.3.5.

Another possible indicator would be to consider only the smallest eigenvalue of $[G_{12}][G_{12}]'$, which is a square matrix regardless of the dimension of $[G_{12}]$. Matrices are non-invertible if and only if they have a zero eigenvalue (Johnson, 1970). Considering this, a near zero eigenvalue might indicate that the matrix is near singular. As can be seen in Figure 16, this also fails to correspond to changes in modified MTF.

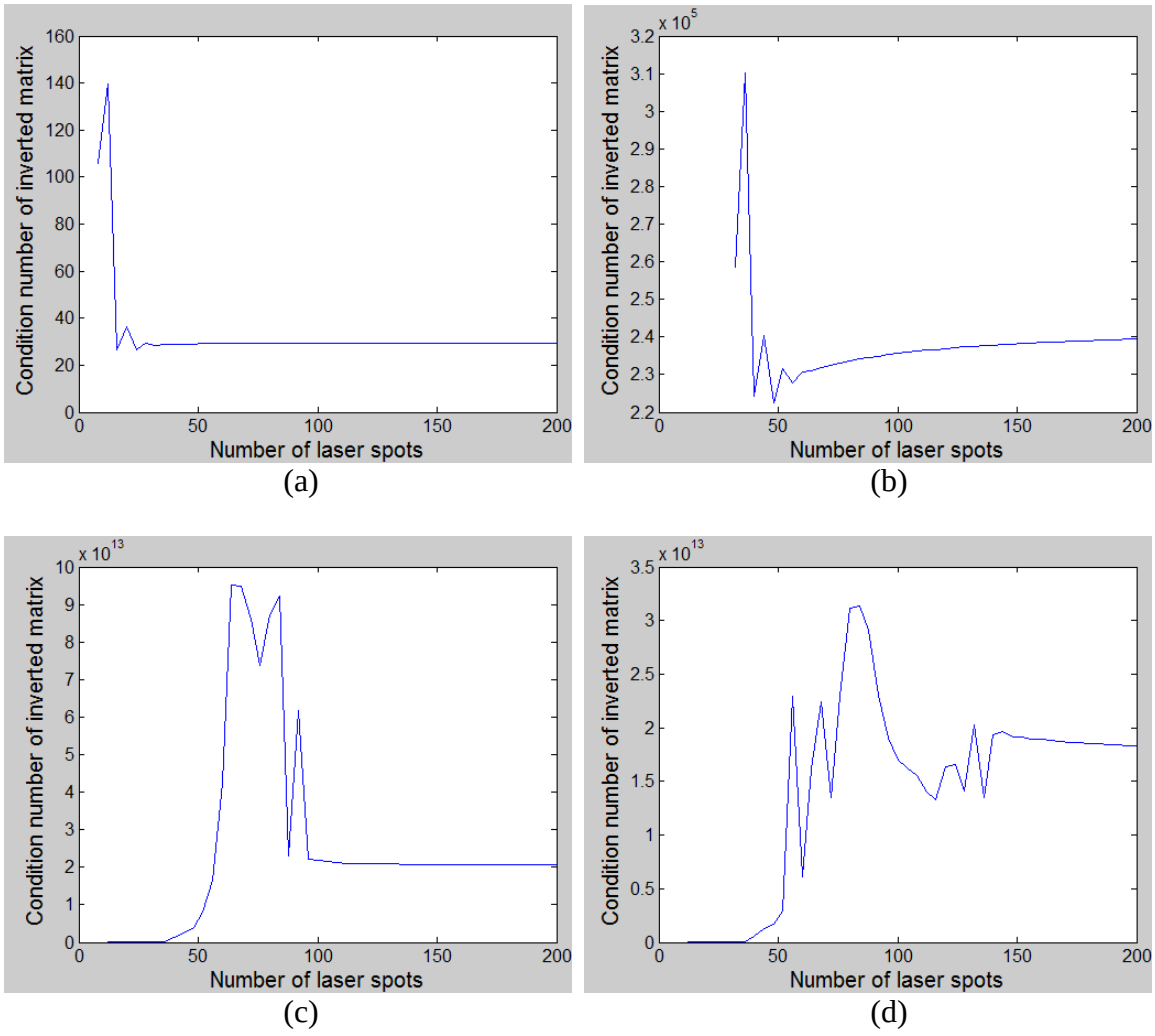

Figure 15. Condition number as a function of number of laser spots for (a) 2x2, (b) 4x4, (c) 8x8 and (d) 16x16 resolutions.

Neither the condition number nor the minimum eigenvalue of this matrix correspond to the changes in modified MTF. While there may be some other value derived from this matrix to indicate the ideal number of laser spots, it has not been found. As a result determining the ideal number of laser spots for a specific geometry requires an exhaustive simulation prior to beginning the physical setup.

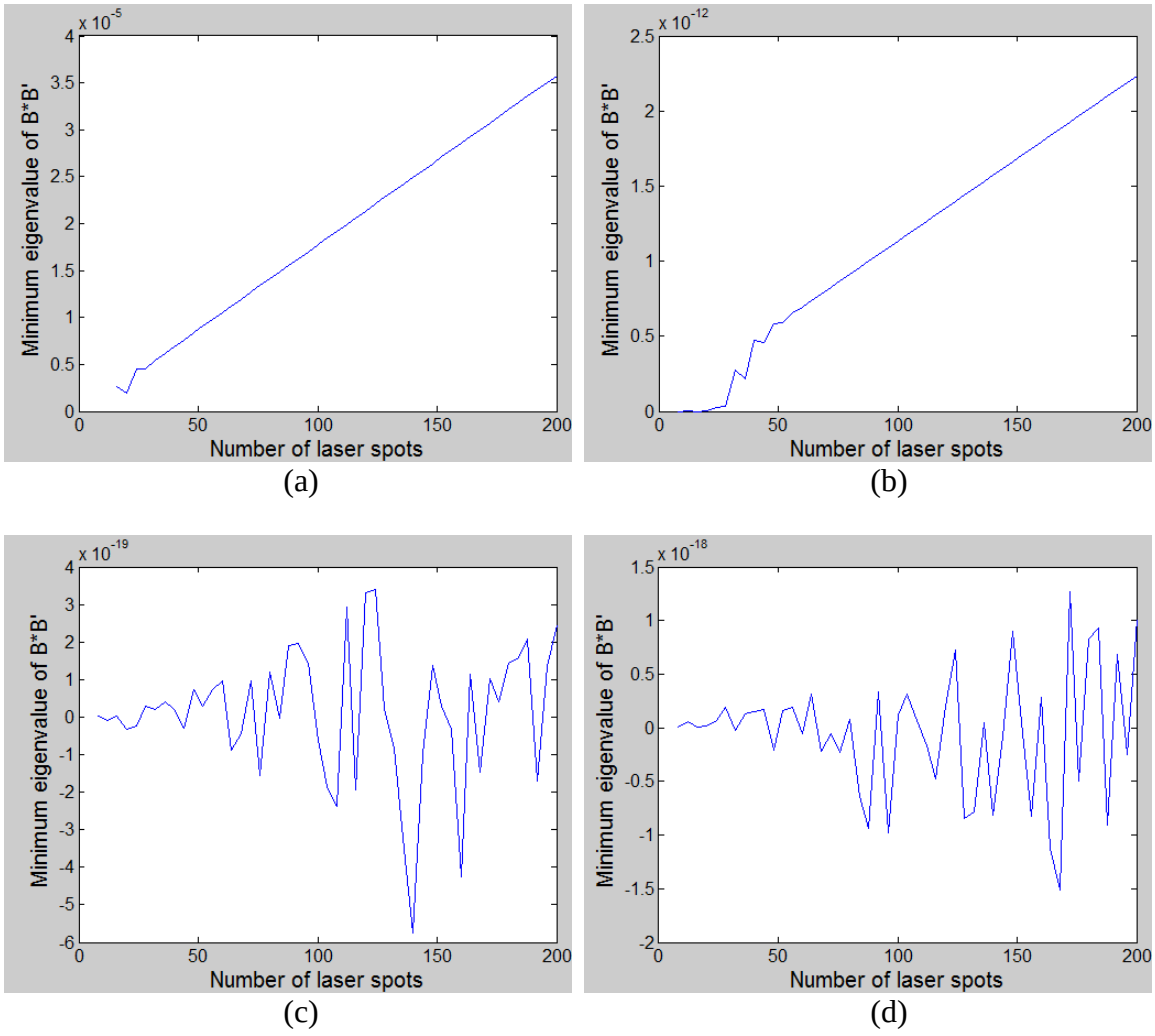

Figure 16. Minimum eigenvalue as a function of number of laser spots for (a) 2x2, (b) 4x4, (c) 8x8 and (d) 16x16 resolution.

4.2.3 Testing Laser Spots at Differing Distances from Object

Another factor which can be varied is the dimensions of the square pattern of laser spots centered at a point on S1 directly beneath the hidden object, hereafter denoted as C. The ideal location is not with the sides of this square as close to C as possible. As these laser spots move further from C, it initially causes successive laser spot location to result

in a greater change in geometry between the laser spot location and object location, thereby contributing values to the $[G_{12}]$ matrix which makes it less singular. Simulation was used to determine at which perpendicular distances from this center point C the modified MTF was maximized, with examples shown in Figures 17 and 18.

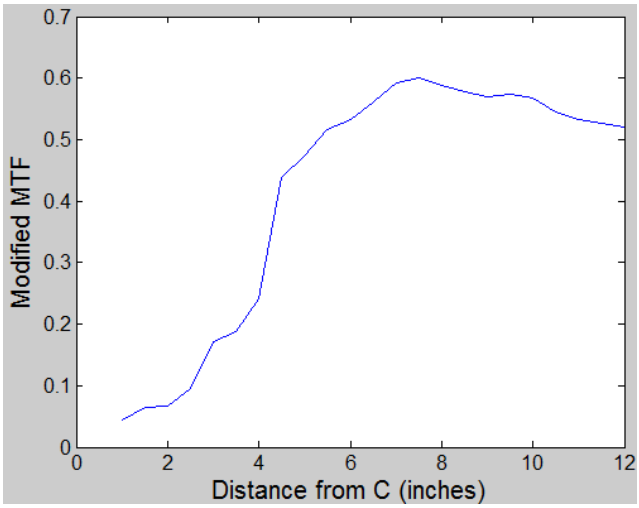

Figure 17. Modified MTF as a function of laser spot distance from C for an 8x8 object at 8x8 resolution with 100 laser spots.

One possible reason for the general trend shown in Figure 17 again involves the invertibility of the matrix involved in these calculations. When the same number of laser spots is put into a smaller perimeter as occurs when the dimensions of a rectangle are decreased, they become closer to one another. Since each column of this matrix represents the geometric relationship of a single laser spot on surface 1 to all points on surface 2, the matrix can become nearly singular if the laser spots are not separated by an appropriate distance.

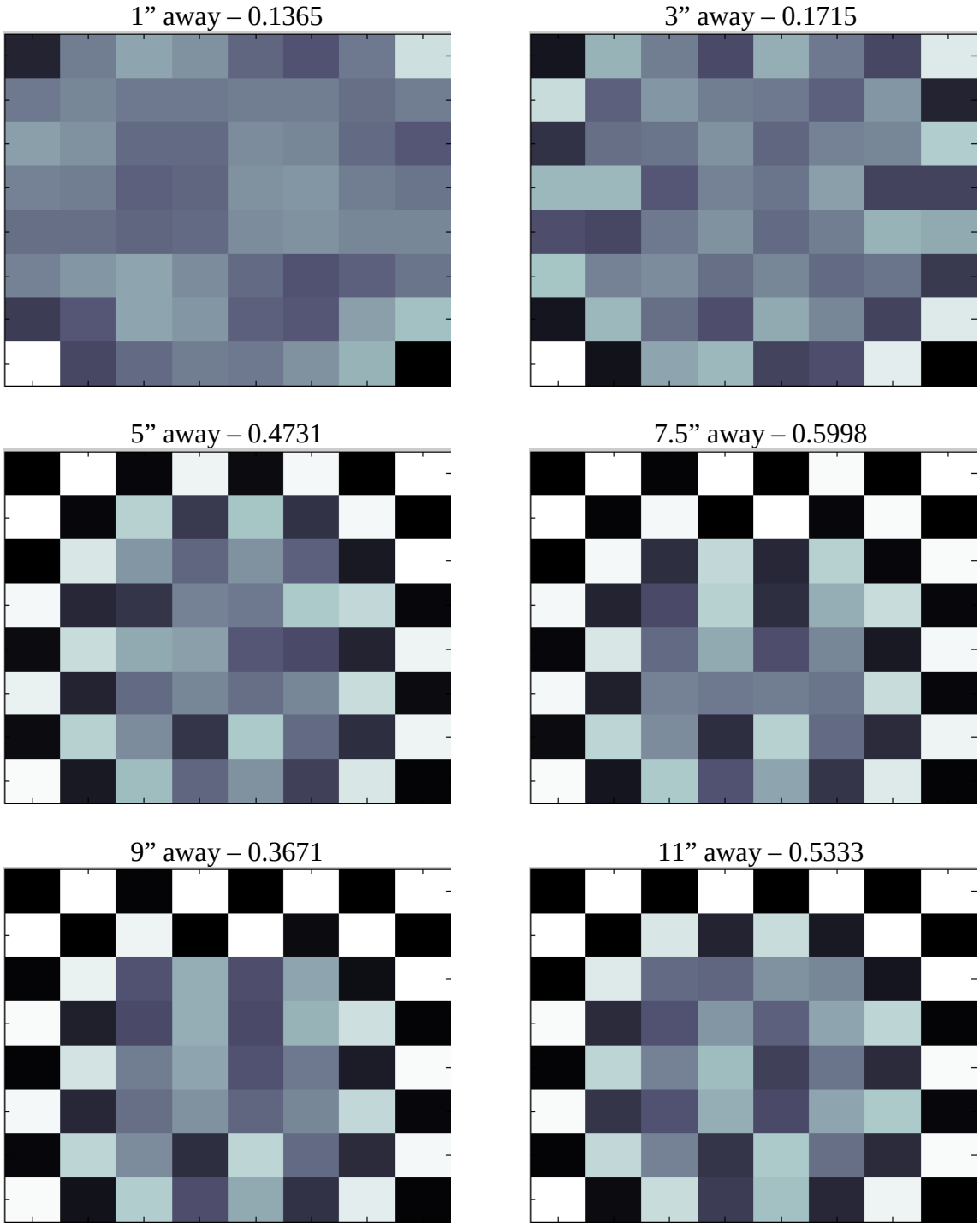

Figure 18. Recovered images for 8x8 object at 8x8 resolution with 100 laser spots at varying distances from C.

This is of particular interest when considering the horizontal lines of laser spots across surface 1. A cross-sectional view of the experimental setup is shown in Figure 19, which allows for the calculation of the basic relationship between these lines of laser spots and the various x-direction lines of the hidden object.

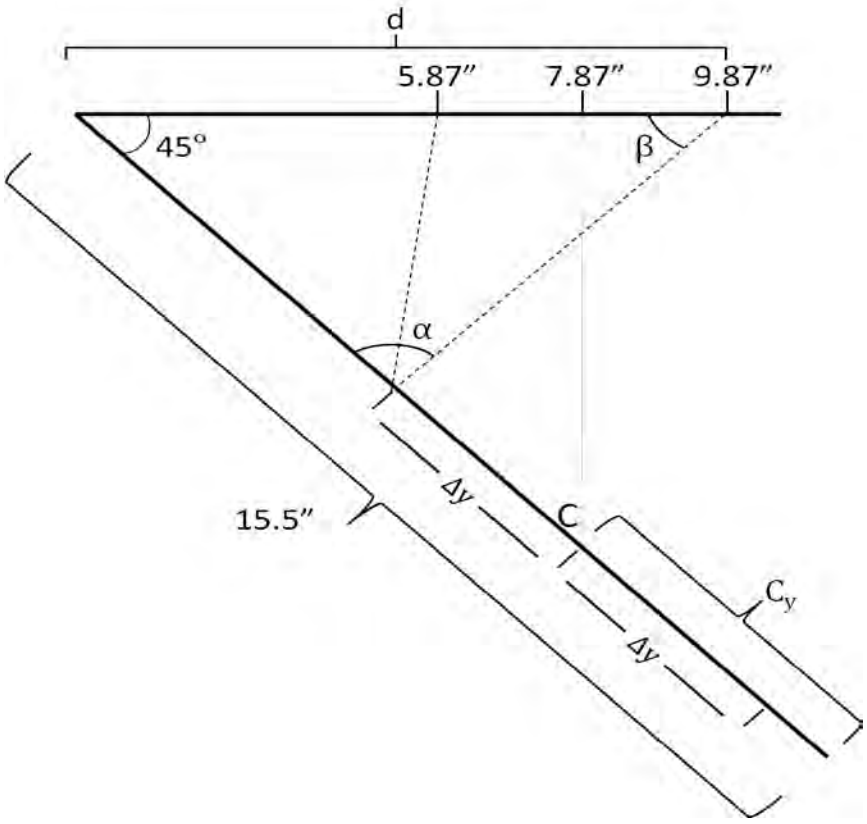

Figure 19. Cross-section of setup used in experimental and simulated trials.

The law of sines gives

$$\frac{\sin(\alpha)}{\mathrm{d}} = \frac{\sin(\beta)}{15.5-(\mathrm{C_y}+\Delta\mathrm{y})} \qquad (4.3.3.1)$$

where C_y is the y-coordinate of the point C, here 4.375", and d and Δy are as shown in Figure 19. Given that $\beta = 135^{\circ} - \alpha$, α can be defined in terms of C_y, Δy and d with

$$\alpha = \operatorname{arccot}\left(\sqrt{2}\,\frac{15.5-(C_y+\Delta y)}{d} - 1\right). \qquad (4.3.3.2)$$

The angle from the lower horizontal line of spots is given by the same expression except with $C_y + \Delta y$ replaced by $C_y - \Delta y$.

From Figure 17, the max modified MTF with a rectangular layout for an 8x8 object with 8x8 desired resolution occurs when the laser spots are 7.5" from C. By using Equation (4.3.3.2) to solve for α, it is possible to solve for simplified versions of θ_{s12}, θ_{d12} and R_{12} for the flattened cross-section, denoted as Θ_{s12}, Θ_{d12} and r_{12}. Letting $K = \cos\Theta_{s12}\cos\Theta_{d12}/r_{12}^2$, the geometric term in this flattened cross-section, allows for comparison of this quantity between different laser spot positions, as seen in Tables 2, 3 and 4.

Table 2. K between horizontal lines of laserspots and rows of hidden object with laser spots in square pattern with edges 7.5" from C.

	Row of Hidden Object (Row 1 is rear-most row, Row 8 is front-most)								Ratio
	1	2	3	4	5	6	7	8	
K for lower line of spots	0.0011	0.0013	0.0015	0.0017	0.0019	0.0021	0.0024	0.0026	2.262
K for upper line of spots	0.0301	0.0227	0.0173	0.0134	0.0105	0.0084	0.0068	0.0055	5.474
Ratio	26.29	17.21	11.51	7.87	5.50	3.93	2.86	2.12	

Table 3. *K* between horizontal lines of laserspots and rows of hidden object with laser spots in square pattern with edges 1" from C.

	Row of Hidden Object (Row 1 is rear-most row, Row 8 is front-most)								Ratio
	1	2	3	4	5	6	7	8	
K for lower line of spots	0.0059	0.0067	0.0075	0.0084	0.0091	0.0097	0.0101	0.0104	1.787
K for upper line of spots	0.0113	0.0126	0.0137	0.0146	0.0151	0.0153	0.0152	0.0148	1.354
Ratio	1.93	1.88	1.82	1.75	1.67	1.58	1.50	1.41	

Table 4. *K* between horizontal lines of laserspots and rows of hidden object with laser spots in square pattern with edges 11" from C.

	Row of Hidden Object (Row 1 is rear-most row, Row 8 is front-most)								Ratio
	1	2	3	4	5	6	7	8	
K for lower line of spots	0.0006	0.0007	0.0008	0.0009	0.0010	0.0011	0.0012	0.0013	2.240
K for upper line of spots	0.0003	0.0002	0.0002	0.0001	0.0001	0.0001	0.0001	0.0001	3.968
Ratio	2.08	3.02	4.29	5.95	8.10	10.83	14.25	18.48	

As can be seen from the ratios in the far right column, which relate the largest and smallest values of *K* for a given line of laser spots, the variation in flux returned from different rows of the object is greatest when the line of laser spots is located 7.5" from the center point C. Additionally, for this setup, the lower and upper horizontal lines of laser spots also shows greater differences at 7.5" than the other distances considered. These traits combine to give the matrix more variation, which makes it less singular and more invertible, resulting in improved image quality.

4.2.4 Testing Differing Layout of Laser Spots

None of the previous examples were able to achieve a modified MTF of greater than 0.6 and had large areas in the middle of the image which were not well resolved. One of the controllable variables which makes the biggest difference in eventual image quality is the layout of the laser spots. As an example, in Figure 18, the image acquired using lines of laser spots 5" from point C had a modified MTF value of 0.4731. Merely by adding a slight stagger to the position of these spots, while keeping the number and general position the same, the MTF can be increased to 1.00, as shown in Figures 20 and 21. The red dots in Figure 20 (right) correspond to the experiment without stagger and to the red line in Figure 20 (left), while blue corresponds to the experiment with stagger.

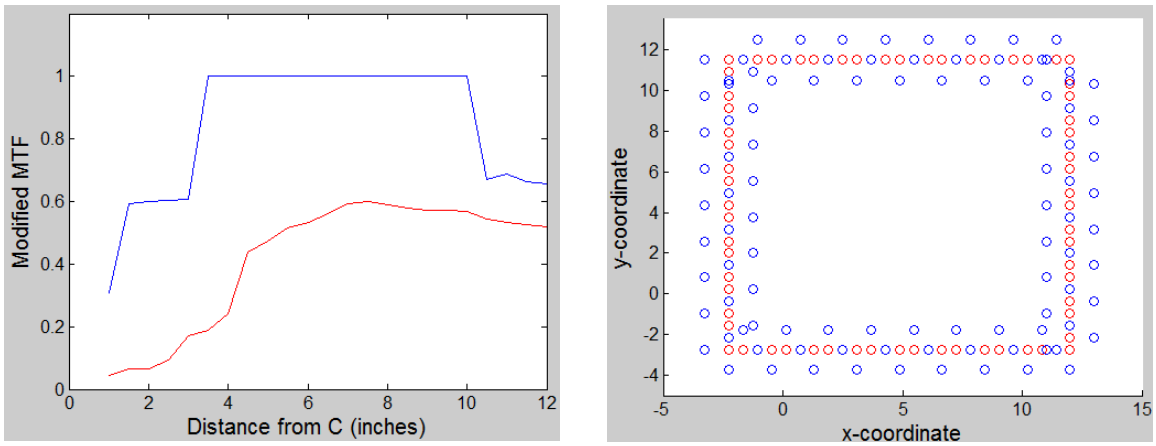

Figure 20. (Left) Modified MTF as a function of distance from C for two different patterns of laser spots; (Right) Laser spot patterns used.

Marked improvements such as this are accomplished in nearly every case by staggering the laser spots as shown in Figure 20. The top of Figure 21 shows the contour

maps of $[G_{12}]$, the matrix requiring inversion, for an 8x8 object with 8x8 resolution, with the resulting indirect images placed underneath. The images on the left are accomplished without stagger and correspond to the red portions of Figure 20, while those on the right make use of staggered laser spot location and correspond to the blue portions of Figure 20. Similar to the image improving as the laser spots initially move away from the field of view on surface 1/3 it is possible this is a result of the matrix simply becoming less singular due to increased variation in the position of the laser spots. This theory is supported by the top images in Figure 21, but further study is still needed on this matter.

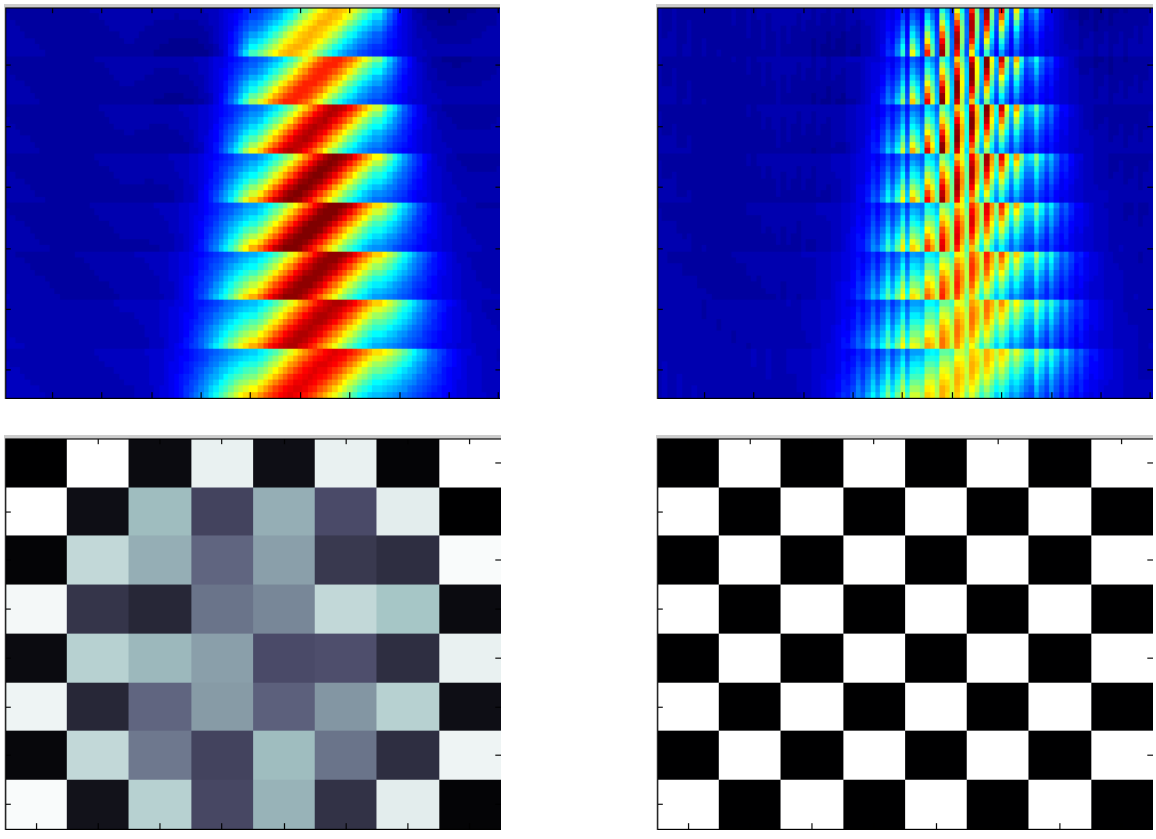

Figure 21. (Top) Contour map of matrix $[G_{12}]$ and (bottom) resulting images. Left is without stagger, right is with stagger of laser spot layout.

4.2.5 Effect of Small Error in Measurement

By adjusting the placement, pattern and number of spots, it is theoretically possible to get a perfect copy of the object as an indirect image, as shown in simulation. It is important, however, to note that real-world conditions are not ideal, and there will likely be some systemic error in those cases. The extremely large condition numbers of matrices to be inverted make this a particularly important case to consider. Large condition numbers for the matrix X means that when solving $AX = B$ for A, even small errors in B result in large errors in A (Zielke, 1983).

To determine the effect that detection noise or other systematic uncertainties can have on a matrix approach to indirect photography, Figure 22 shows the modified MTF of the recovered indirect image at various resolutions, and Figures 23 and 24 show the recovered image, after a random normally distributed percent error with varying standard deviations has been individually introduced to each pixel in the photographed intensity.

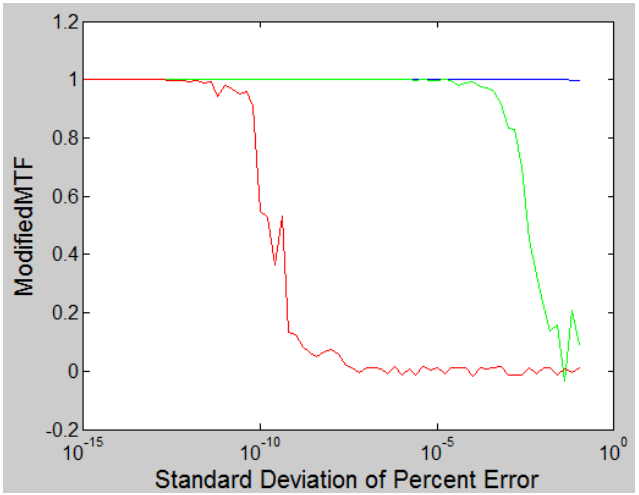

Figure 22. Modified MTF of 2x2 objects at varying resolution (Blue - 2x2, Green - 4x4, Red 8x8) with 120 staggered laser spots and lines 6" from C.

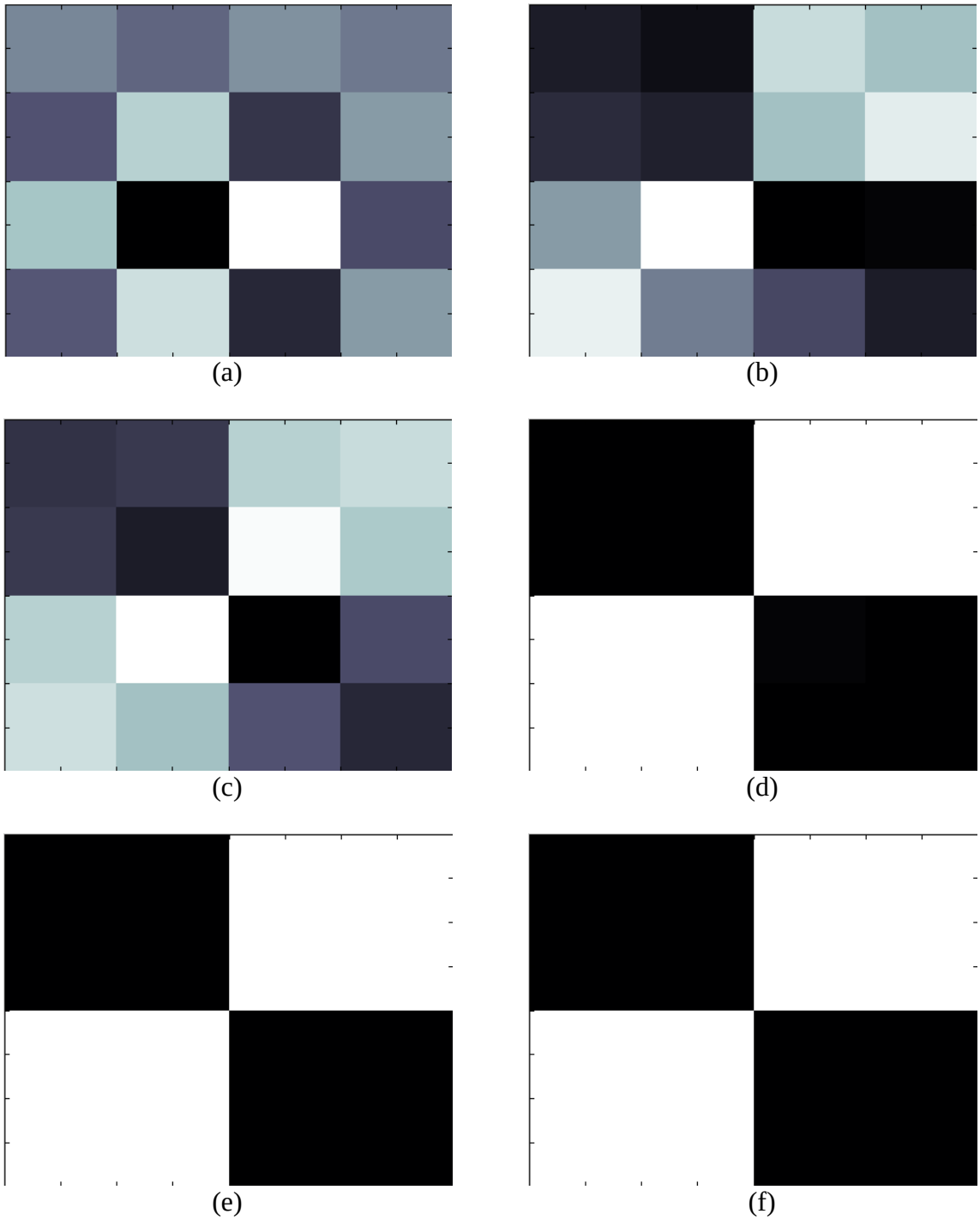

Figure 23. Recovered indirect images for 2x2 object at 4x4 resolution with intensity added percent error with standard deviation of (a) 10, (b) 1, (c) 0.1, (d) 1e-2, (e) 1e-3 and (f) No error.

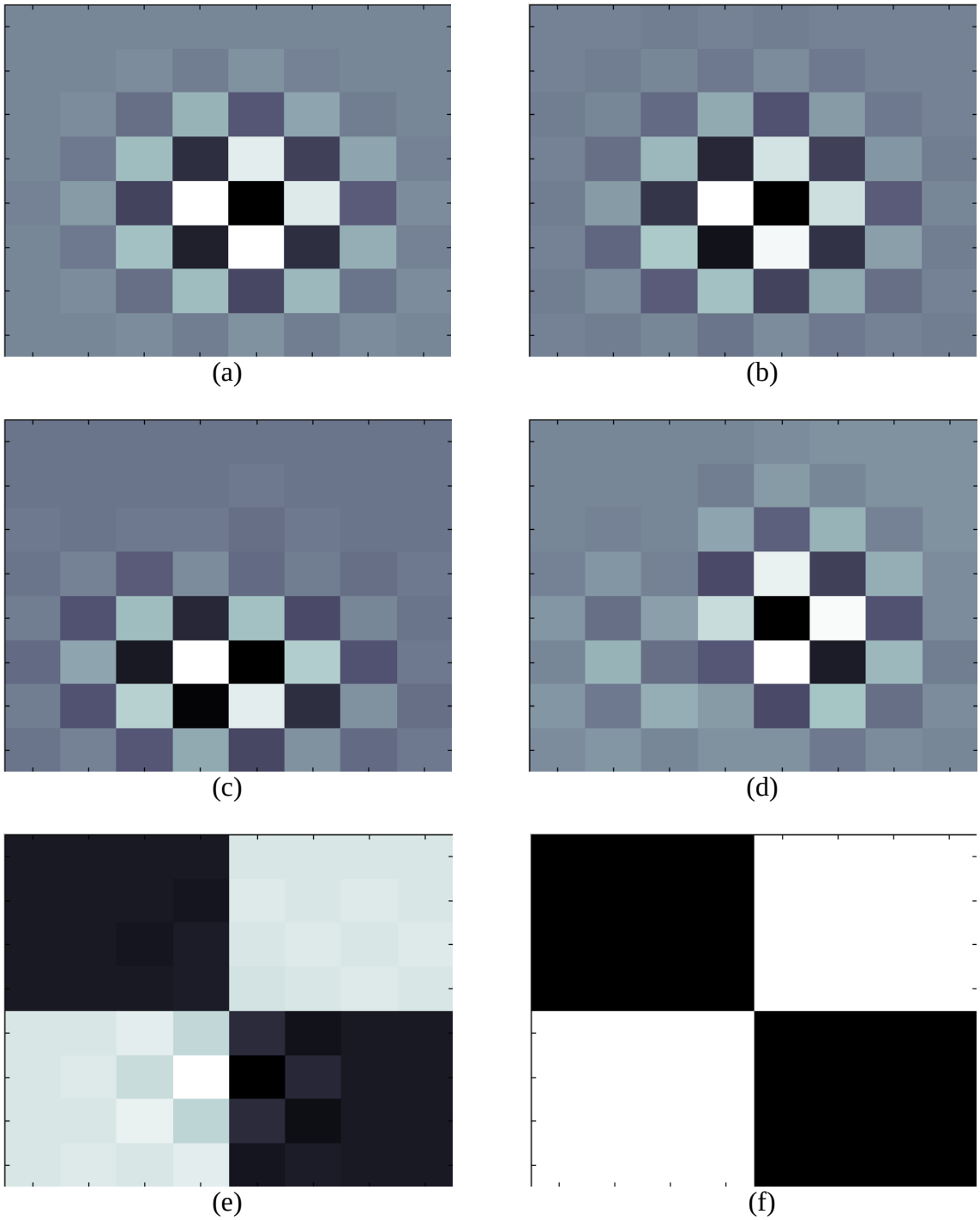

Figure 24. Recovered indirect images for 2x2 object at 8x8 resolution with intensity added percent error with standard deviation of (a) 1, (b) 1e-2, (c) 1e-4, (d) 1e-6, (e) 1e-8 and (f) 1e-10.

The recovered indirect images with 2x2 resolution are not included since these tended to be very accurate regardless of the error in camera measurement. This is a result of the much lower condition numbers associated with the matrices used in resolving images at this resolution (see Figure 15). From this, it is clear that a higher desired resolution will require less error in the measurements recorded by the camera in order to maintain a recognizable image. Additionally, this issue can be somewhat diminished by minimizing the condition number of the matrix to be inverted. This can be accomplished by varying the number, position and layout of the laser spots, and can be quickly performed in simulation before beginning with an experimental setup.

4.3 Investigative Questions Answered

The primary purpose of this work was to determine if it is possible to perform indirect photography by using matrices. While this could not previously be verified experimentally due to flawed data, the simulated scenarios provide strong evidence that this can be mathematically accomplished. The question of the best mathematical method for this case was also resolved, in favor of using the Moore-Penrose pseudoinverse for the required matrix inversion.

Trends which determine the quality of the recovered image as a function of the number, location and pattern of the laser spots used to illuminate surface 1 were sought. While no indicator was found which corresponded to an ideal setup, it was discovered that a relatively small number of laser spots (less than 130) was required in most cases with this setup and that continuing to add more after approximately 120 never markedly improved the final result. While this will likely vary according to the experimental setup,

this does indicate that increasing the number of laser spots does increase the recovered indirect image quality, but that this cannot be continued indefinitely. Additionally, the question of what other methods could be used to improve the image was answered by showing the increase in MTF associated with moving the laser spots further from the field of view on surface 1/3 and by adding some variation to the pattern of the laser spots. These results are tempered by the very high level of accuracy required by the camera in order to produce recognizable images.

4.4 Summary

By adjusting a combination of variables, it is possible to resolve 2x2 checkerboards at nearly any resolution, 4x4 checkerboards at up to at least 32x32 resolution, and 8x8 checkerboards at 8x8 resolution in the given setup. As distances and angles between surfaces change, it is likely that these values will change. However the general trends will remain and the overall ability to indirectly image otherwise hidden objects using a matrix formulation appears to be mathematically feasible, though it requires very accurate equipment.

5. Conclusions and Recommendations

5.1 Chapter Overview

This chapter contains the conclusions of this initial research into matrix-based indirect imaging techniques, as well as the significance of these results. While this research was accomplished with specific geometry and hidden objects, these conclusions include several trends which hold for matrix-based indirect imaging techniques in general. Also included is a brief overview of some of the research that has either been opened up by this work or remains to be done.

5.2 Conclusions of Research

This work has effectively demonstrated that an algorithm using the Moore-Penrose pseudoinverse for matrix inversion can be used to recover information about a hidden object using an indirect photography technique. Though this was accomplished with the assumption that the visible surface was Lambertian, this process will still work if this is not the case, so long as the BRDF of the surface is known. Additional conclusions which can be drawn include that the most important factor in this case was the pattern used to determine the coordinates where the laser spots were on the visible reflecting surface. Increasing the actual number of laser spots tended to cause a quick initial increase in resolved image quality, but it should be noted that continuing to add more did not have any positive influence after a certain point. As a result, other methods, such as varying the layout of these spots, must be pursued to increase image quality. This becomes particularly important when the data from the camera becomes noisy or

uncertain, since it is then very important to minimize the condition number of the matrix to be inverted. It was also determined that while the modified MTF serves as an excellent indicator of this image quality, it is important to ensure that the values used in its calculation are physical, rather than an unphysical result of mathematical manipulation.

5.3 Significance of Research

While indirect photography has previously been introduced and demonstrated, this research provides an alternative method which can be pursued. Using matrices and a setup in which the position of the laser spot is free to move independently from the camera FOV also increases the general practicality of indirect photography by reducing the physical restraints on where it can be applied. A large unbroken, uniform surface for laser reflection and camera FOV is no longer required as was previously the case. This initial work with the matrix formulation of the transport involved in indirect photography also opens the path for further research into the general form of the matrices associated with other experimental setups, eventually allowing for indirect photography to be used in situations which do not have a known geometry. Indirect photography itself has a great deal of significance, particularly within the intelligence community and emergency services, as a means to identify and locate items of importance.

5.4 Recommendations for Future Research

There are several questions raised by this research, all of which are deserving of future research. One important question which remained unanswered is what indicators,

if any, correspond to an idealized indirect photography setup. While this must be a function of the matrix which is inverted, this research was unable to find any quantity which appropriately described the invertibility of this non-square matrix. Finding such a value would greatly reduce the time needed for simulations and preparations once this process has reached a point where it can be applied for practical purposes.

In a similar vein, before indirect photography can be effectively used, it is important that further research be done into the general form of the matrices involved in indirect photography. There are several important facets to this. While matrices were considered for one particular setup in the course of this research, it will be essential to research how these matrices change as the geometry changes in order to create approximate matrices for use when the specific geometry is not known. In conjunction with this, it will also be important to understand which parts of the geometry are most important to accurately model or approximate, and how error in those values affects the overall result. Mathematical research should also be conducted into which factors can contribute to minimizing the condition number of the matrix resulting from the geometric relations between fixed points (resolution elements on S2) and user-defined locations (laser points on S1).

Finally, it should be noted how much of a difference the layout and pattern of the laser spots on surface 1 can make. In this paper, these were limited to rectangular patterns and rectangular patterns with small offsets. As there are infinitely many different possible variations of patterns which can be used, it is recommended that a method be researched to determine the best possible pattern for these laser spots. This

will require that it first be determined why some patterns are able to achieve more impressive results than others, and then expand this to maximize that effect.

5.5 Recommendations for Action

Research into indirect photography remains in its infancy, and both the theory and application need to be further developed before it can be put into practical use. Another hindrance to currently applying these techniques is the current state of computing power. Until this increases, this can only be used for delayed information-gathering. At this time, the best course of action is for information regarding indirect photography to be disseminated to various academic institutions for further work and research, with a particular emphasis on physics, mathematics, and image processing.

5.6 Summary

Indirect photography is still in the early stages of development and much more research needs to be accomplished before it can be used in real world application. However, this document provides the basis for that research to be conducted using a matrix-based data reduction technique, beginning with a number of simplifying assumptions and slowly removing these until the technique of indirect photography becomes practical and useful.

Appendix A – Representative Example of Simulation Code

This code is a representative example of the simulation code used to test the effect of varying different parameters. In this case, the parameter which is varied is the number of laser spots. The user inputs the spatial frequency of the checkerboard, the number of pixels for each dimension of the camera, the desired resolution and the range of number of laser spots to consider. Additionally, within the code the offset from the center point C can be modified, as well as whether or not there is stagger. The output of this code gives the object, a vector containing the number of laserspots, and corresponding vectors with the modified MTF as well as the condition number, and minimum eigenvalue of the matrix $[G_{12}]$. Other similar code is used to vary the distance of laser spots lines from point C, the method of inversion, and the amount of error in the camera measurement. Because of the similarity, copies of this code are not included here.

```
function [Object LaserSpots MTF CNum MinEig]=InImSimB2(CheckSize,
CamRow, CamCol, Resolution, MinSpots, MaxSpots)

%% Define Object BRDF
ObjectRows=CamRow*CamCol;
ObjectCols=(Resolution)^2;
Object(ObjectRows,ObjectCols)=0;
Restart=Resolution^2/CheckSize;
for i=1:ObjectCols
    if mod(floor(i/(Restart+.001)),2)==0;   %if column corresponds to
                                            odd 'row' of the object
                                            checks
        if mod(floor(i/(Resolution/CheckSize+.001)),2)==1;
            Object(:,i)=1;
        end
    else
        if mod(floor((i)/(Resolution/CheckSize+.001)),2)==0;
            Object(:,i)=1;
        end
    end
end
```

```
ObjectAvg=mean(Object);
ObjView(Resolution,Resolution)=0;  %Pre-allocate for speed

for i=1:(Resolution)
    for j=1:(Resolution)
        ObjView(i,j)=ObjectAvg((i-1)*(Resolution)+j);
    end
end

figure(1)
colormap(bone)
imagesc(ObjView)

%% Define S2 positions
L1y=15.5;
x2min=3;
x2max=7;
x2step=(x2max-x2min)/(Resolution);
CenterX=5;

%d2 is measured from rear of surface2
d2min=5.86764;
d2max=9.86764;
d2step=(d2max-d2min)/(Resolution);

x2=((x2min+x2step/2):x2step:(x2max-x2step/2));
d2=(d2min+d2step/2):d2step:(d2max-d2step/2);

z2=(d2)./sqrt(2);
y2=L1y-z2;
CenterY=L1y-7.86764*sqrt(2);

%% Define S3 positions
x3min=3.25;
x3max=6.5;
x3max=(x3max-x3min)+x3min;
x3step=-(x3max-x3min)/(CamCol-1);

y3top=6;
y3bottom=2.75;
y3bottom=y3top-(y3top-y3bottom);
y3step=(y3top-y3bottom)/(CamRow-1);

x3=x3max:x3step:x3min;
y3=y3bottom:y3step:y3top;

%% Create D23 matrix
D23(length(x3)*length(y3),length(x2)*length(y2))=0; %Preallocate for
                                                      speed
```

```
for h=1:length(y2)
    for i=1:length(x2)
        for j=1:length(y3)
            for k=1:length(x3)
                  D23(k+(j-1)*length(x3),i+(h-1)*length(x2))=
                        (z2(h)*sqrt((1/2)*((y3(j)-y2(h))^2+z2(h)^2)))/
                        (((x3(k)-x2(i))^2+(y3(j)-y2(h))^2+z2(h)^2)^(2))
            end
        end
    end
end

for b=1:MaxSpots-MinSpots+1;
    LaserSpots(b)=b+MinSpots-1;

x1min=CenterX-6;
x1max=CenterX+6;
x1step=(x1max-x1min)/(LaserSpots(b)-1);
x1vector=x1min:x1step:x1max;

y1min=CenterY-6;
y1max=CenterY+6;
y1step=(y1max-y1min)/(LaserSpots(b)-1);
y1vector=y1max:-y1step:y1min;

x1(4*LaserSpots)=0;
y1(4*LaserSpots)=0;

for i=1:LaserSpots(b)
    if mod(i,3)==0
        Offset=0;
    elseif mod(i,3)==1
        Offset=-1;
    else
        Offset=1;
    end
    x1(i)=x1vector(i);
    x1(i+LaserSpots(b))=x1max+Offset;
    x1(i+2*LaserSpots(b))=x1vector(LaserSpots(b)+1-i);
    x1(i+3*LaserSpots(b))=x1min+Offset;
    y1(i)=y1min+Offset;
    y1(i+LaserSpots(b))=y1vector(LaserSpots(b)+1-i);
    y1(i+2*LaserSpots(b))=y1max+Offset;
    y1(i+3*LaserSpots(b))=y1vector(i);
end

figure(2)
plot(x1,y1);
length(x1);

D12(length(x2)*length(y2),length(x1))=0;  %Preallocate for speed
```

```
for i=1:length(x1)
    for j=1:length(y2)
        for k=1:length(x2)
            Radius(k+(j-1)*length(x2),i)=
                  sqrt((x1(i)-x2(k))^2+(y1(i)-y2(j))^2+z2(j)^2);
            CosS(k+(j-1)*length(x2),i)=
                  z2(j)./Radius(k+(j-1)*length(x2),i);
            CosD(k+(j-1)*length(x2),i)=
                  sqrt(1/2)*(y1(i)-y2(j)+z2(j))./
                  Radius(k+(j-1)*length(x2),i);
            D12(k+(j-1)*length(x2),i)=
                  CosS(k+(j-1)*length(x2),i).*
                  CosD(k+(j-1)*length(x2),i)./(Radius(k+(j-1)*
                  length(x2),i).^2);
            D12(k+(j-1)*length(x2),i)=
                  (z2(j)*sqrt((1/2)*((y1(i)-y2(j))^2+z2(j)^2)))/
                  (((x1(i)-x2(k))^2+(y1(i)-y2(j))^2+z2(j)^2)^(2));
        end
    end
end

%% Cleanup unneeded variables
clear ObjView ObjectAvg
clear Alpha Gamma1 Gamma2 GammaStepB GammaStepT GammaVB GammaVT
clear LGV LGVB LPV Phi1 Phi2 PhiStep PhiV
clear Sigma XOrigin YOrigin dm0 h i j k s v w L1y L2k d2min d2max
clear d2step x2min x2max x2step x3step y3step
clear x3 y3 CamCol CamRow

%% Calculate Intensity
Intensity=(Object.*D23)*D12;

%% Reverse Calculate BRDF of Object
BRDF=(pinv(D12')*Intensity')'./D23;

for i=1:length(BRDF(1,:))
    BRDFAvg(i)=sum(BRDF(:,i))/length(BRDF(:,1));
end

minBRDF=min(BRDFAvg);
maxBRDF=max(BRDFAvg);

BRDFAvg=(BRDFAvg-minBRDF)/(maxBRDF-minBRDF);

for i=1:length(x2)
    for j=1:length(d2)
        BRDFMat(i,j)=BRDFAvg((i-1)*length(d2)+j);
    end
end

%figure(3)
%colormap(bone)
```

```
%imagesc(BRDFMat)

DarkSum=0;
for i=1:ObjectCols
    if mod(floor(i/(Restart+.001)),2)==0;   %if column corresponds to
                                             odd 'row' of the object
                                             checks
        if mod(floor(i/(Resolution/CheckSize+.001)),2)==1;
            DarkSum=DarkSum+BRDFAvg(:,i);
        end
    else
        if mod(floor((i)/(Resolution/CheckSize+.001)),2)==0;
            DarkSum=DarkSum+BRDFAvg(:,i);
        end
    end
end

LightSum=sum(sum(BRDFMat))-DarkSum;
MTF(b)=(DarkSum-LightSum)/(sum(sum(BRDFMat)));
CNum(b)=norm(D12)*norm(pinv(D12));
MinEig(b)=eigs(D12*D12',1,'sm');

clear Intensity BRDF D12 Radius CosS CosD
end

figure(1)
plot(LaserSpots*4,MTF)
set(gca,'fontsize',12)
xlabel('Number of laser spots','fontsize',15)
ylabel('Modified MTF','fontsize',15)

figure(2)
plot(LaserSpots*4,CNum)
set(gca,'fontsize',12)
ylabel('Condition number of inverted matrix','fontsize',15)
xlabel('Number of laser spots','fontsize',15)

figure(3)
plot(LaserSpots*4,MinEig)
set(gca,'fontsize',12)
ylabel('Minimum eigenvalue of B*B''','fontsize',15)
xlabel('Number of laser spots','fontsize',15)

end
```

6. Bibliography

Dereniak, E., & Boreman, G. (1996). *Infrared Detectors and Systems.* New York, NY: John Wiley & Sons.

Driggers, R., Cox, P., & Edwards, T. (1999). *Introduction to Infrared and Electro-Optical Systems.* Boston, MA: Artech House.

Erceg, V., Soma, P., Baum, D., & Paulraj, A. (2002). Capacity obtained from multiple-input multiple-output channel measurements in fixed wireless environments at 2.5 GHz. *IEEE International Conference on Communications, 2002*, (pp. 396-400). New York.

Ferrel, S., Schafer, J., & Powell, N. (2011). *Matrix Determination of BRDF of Hidden Object via Indirect Photography.* Unpublished. Air Force Institute of Technology. Dayton, OH.

Hoelscher, M. G. (2011). *Restoration of Scene Information Reflected from Non-Specular Information.* WPAFB: Air Force Institute of Technology.

Hoelscher, M. G., & Marciniak, M. A. (2010). Restoration of scene information reflected from a non-specular surface., *SPIE 7792*.

Hogban, L., Brualdi, R., Greenbaum, A., & Matthias, R. (2003). *Handbook of Linear Algebra.* Boca Raton, FL: Chapman & Hack/CRC.

Johnson, C. R. (1970). Positive definite matrices. *The American Mathematical Monthly , 77* (3), 259-264.

Leon, S. J. (2005). *Handbook of Linear Algebra: MATLAB Article.* Coimbra, Portugal: University of Coimbra.

Meyer-Spradow, J., & Loviscach, J. (2003). Evolutionary Design of BRDFs. *Proceedings of Eurographics 2003.*

Penrose, R. (1955). A generalized inverse for matrices. *Mathematical Proceedings of the Cambridge Philosophical Society*, (pp. 406-413).

Rayleigh, J. &. (1900). On the law of reciprocity in diffuse reflection. *Philosophical Magazine* , 324-325.

Sen, P., Chen, B., Garg, G., Marschner, S. R., Horowitz, M., Levoy, M., et al. (2005). Dual Photography. *ACM Siggraph 2005.*

von Helmholtz, H., & Southall, J. (1862). *Helmholtz Treatise on Physiological Optics.* Dover.

Zielke, G. (1983, November). Some remarks on matrix norms, condition numbers, and error estimates for linear equations. *Linear Algebra and its Applications , 110,* pp. 29-41.

REPORT DOCUMENTATION PAGE

Form Approved
OMB No. 074-0188

PLEASE DO NOT RETURN YOUR FORM TO THE ABOVE ADDRESS.

1. REPORT DATE *(DD-MM-YYYY)*	2. REPORT TYPE	3. DATES COVERED *(From – To)*
22-03-2012	Master's Thesis	March 2011 – March 2012

TITLE AND SUBTITLE

Matrix Determination of Reflectivity of Hidden Object via Indirect Photography

5a. CONTRACT NUMBER

5b. GRANT NUMBER

5c. PROGRAM ELEMENT NUMBER

6. AUTHOR(S)

Ferrel, Simon S., 2nd Lieutenant, USAF

5d. PROJECT NUMBER
N/A

5e. TASK NUMBER

5f. WORK UNIT NUMBER

7. PERFORMING ORGANIZATION NAMES(S) AND ADDRESS(S)
Air Force Institute of Technology
Graduate School of Engineering and Management (AFIT/EN)
2950 Hobson Way, Building 640
WPAFB OH 45433-7765

8. PERFORMING ORGANIZATION REPORT NUMBER

AFIT/APPLPHY/ENP/12-M05

9. SPONSORING/MONITORING AGENCY NAME(S) AND ADDRESS(ES)

Intentionally Left Blank

10. SPONSOR/MONITOR'S ACRONYM(S)

11. SPONSOR/MONITOR'S REPORT NUMBER(S)

12. DISTRIBUTION/AVAILABILITY STATEMENT
APPROVED FOR PUBLIC RELEASE; DISTRIBUTION UNLIMITED.

13. SUPPLEMENTARY NOTES

14. ABSTRACT

Indirect photography is a recently demonstrated technique which expands on the principles of dual photography and allows for the imaging of hidden objects. A camera and light source are collocated with neither having line-of-sight access to the hidden object. Light from the source, a laser, is reflected off a visible non-specular surface onto the hidden object, where it is reflected back to the initial non-specular surface and collected by the camera. This process may be repeated numerous times for various laser spot positions to yield slightly different camera images due to a variation in the illumination of the object. These images can then be used to construct an "indirect" image of the hidden object. This work provides an alternative method of processing the camera images by modeling this system as a set of transport and reflectance matrices. This approach reduces the required size of the visible scattering surface. Matrix formulation and those parameters shown in simulation to improve indirect image quality as measured by a modified MTF, including the method of matrix inversion, number and pattern of laser spots, are discussed.

15. SUBJECT TERMS
Indirect Photography, Helmholtz Reciprocity, Matrix Inversion

16. SECURITY CLASSIFICATION OF:			17. LIMITATION OF ABSTRACT	18. NUMBER OF PAGES	19a. NAME OF RESPONSIBLE PERSON
a. REPORT	b. ABSTRACT	c. THIS PAGE			Michael A. Marciniak, PhD ADVISOR
U	U	U	UU	69	19b. TELEPHONE NUMBER *(Include area code)* (937) 255-3636, ext 4529 (michael.marciniak@afit.edu)

Standard Form 298 (Rev. 8-98)
Prescribed by ANSI Std. Z39-18